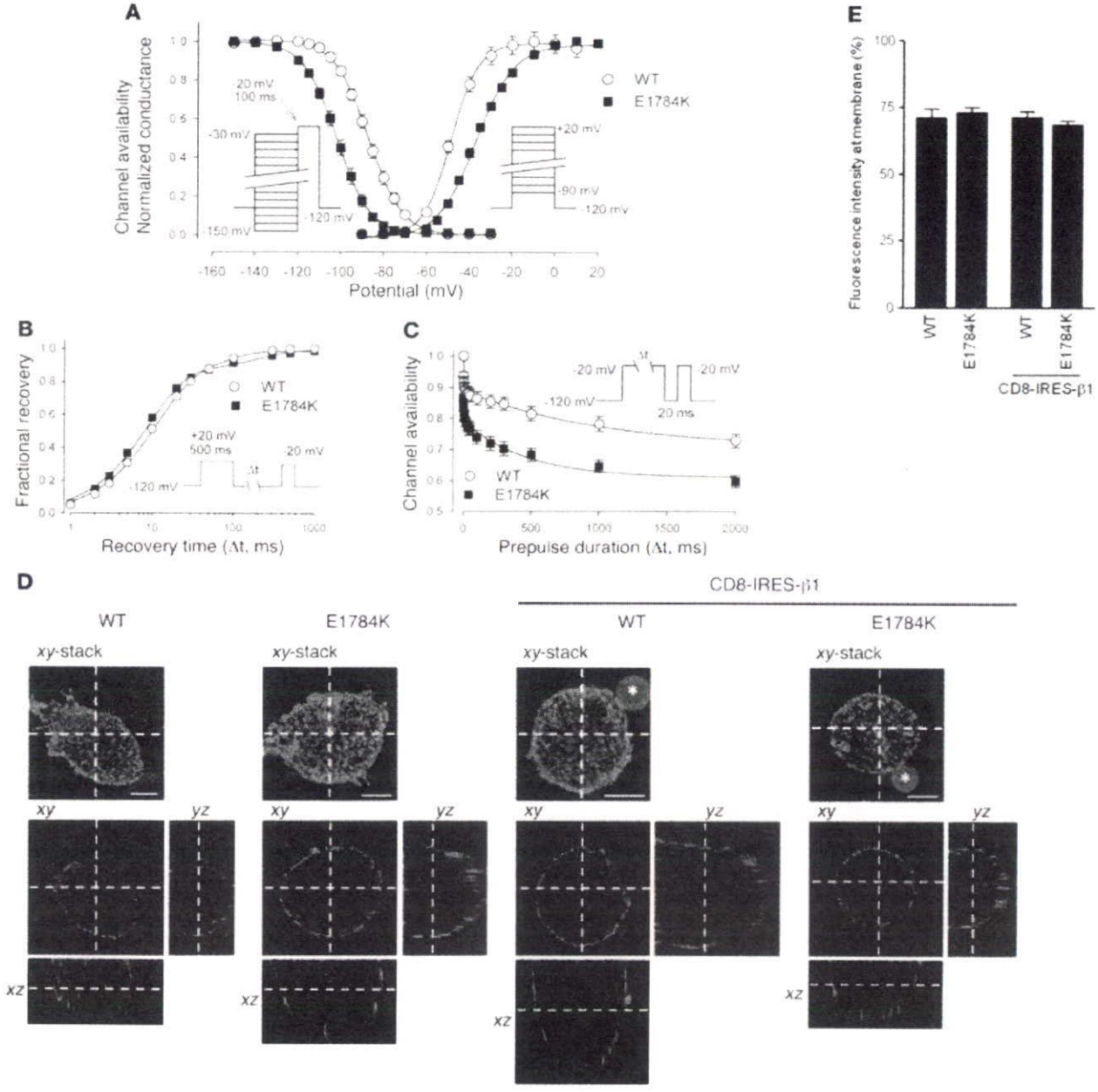

Figure 4

Gating and trafficking properties of E1784K. (**A**) The voltage dependence of steady-state fast inactivation and activation of E1784K, measured with standard pulse protocols shown in insets, were significantly shifted in the hyperpolarizing (−15.0 mV) and depolarizing (+12.5 mV) directions, respectively. (**B**) Recovery from inactivation assessed by the double-pulse protocol was nearly identical between WT and E1784K. (**C**) Slow inactivation, measured by the double-pulse protocol shown in inset, was significantly enhanced in E1784K ($P < 0.05$) in the magnitude of slow inactivation at all prepulse durations from 10 ms to 2,000 ms. (**D**) Cells expressing either FLAG-tagged WT or E1784K in the presence or absence of pCD8-IRES-β1 were immunostained with anti-FLAG antibody. Optical sections of Alexa Fluor 488 (green) were obtained using a confocal laser scanning microscope. Upper and lower panels show the *xy*-stacked image and the *xy* image sliced at *z* axis on the *xz* and the *yz* images, respectively. The *xz* and *yz* images indicate horizontal and vertical sections at the *x* axis and *y* axis on the *xy* image. Asterisks and scale bars in *xy*-stacked images represent anti-CD8 Dynabeads and 5 μm, respectively. Note that both WT and E1784K predominantly localized to the plasma membrane regardless of β1 subunit coexpression. (**E**) Membrane expression of Nav1.5 observed in **D** was quantified as described in Methods. Fluorescence intensity of Nav1.5 staining at plasma membrane, expressed as percentage relative to that of entire cell area, was comparable between WT and E1784K regardless of β1 subunit coexpression.

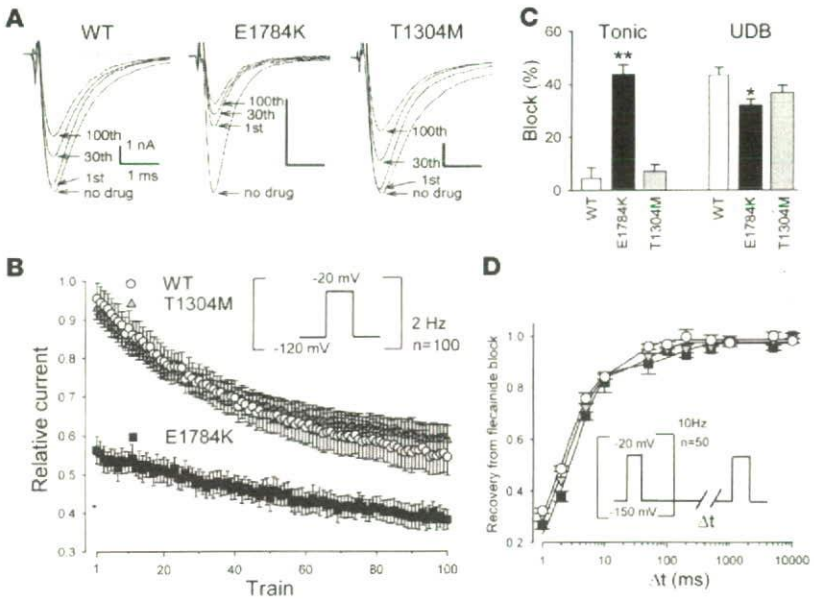

Figure 5

Tonic block and UDB by flecainide. (**A**) Representative current traces of WT, E1784K, and T1304M before and after 10 μmol/l flecainide. A train of 100 pulses (to –20 mV for 20 ms) was applied at 2 Hz from a holding potential of –120 mV. Numbers indicate the first, 30th, and 100th pulse of the 2-Hz train. Zero current levels are indicated by dotted lines. (**B**) Time course of the peak current levels after application of 10 μmol/l flecainide. Peak current levels recorded with each pulse were normalized to the baseline prior to flecainide treatment. (**C**) Tonic block, determined by the first test pulse after application of flecainide, was weak in WT (4.5% ± 4.0%, $n = 5$) and T1304M (7.1% ± 2.7%, $n = 5$; P = NS) but was remarkably enhanced in E1784K (43.7% ± 8.0%, $n = 5$; $^{**}P < 0.001$). Conversely, UDB, determined by the difference between first and 100th pulses relative to the first pulse, was slightly attenuated in E1784K (WT, 43.4% ± 3.0%; E1784K, 32.0% ± 2.2%; $^{*}P < 0.05$), but not in T1304M (36.9% ± 2.7%; P = NS). Net flecainide block at the 100th train was significantly enhanced in E1784K (WT, 45.5% ± 5.0%; E1784K, 61.8% ± 2.5%; $P < 0.01$) but not in T1304M (41.2% ± 3.2%; P = NS). (**D**) Recovery from flecainide block. Cells were held at a potential of –150 mV and superfused with 30 μmol/l flecainide, and a train of 50 pulses (to –20 mV for 20 ms) at 10 Hz was applied to block Na channels. The pulse protocol cycle time was 60 s. Recovery from block was then assessed by a –20-mV test pulse applied after varying the duration of a –150-mV repolarization period (Δt). Peak current was normalized, and the data were fit to a double exponential function.

–37.2 ± 0.9 mV, $n = 13$; $P < 0.001$). For example, conductance elicited by a depolarizing pulse of –30 mV to the maximum conductance was 0.93 ± 0.05 in WT channel but was only 0.66 ± 0.02 in E1784K channel. Both the negative shift of steady-state inactivation and the positive shift of activation reduced channel availability and conductance, respectively, and thus were predicted to decrease Na current during the upstroke of the action potential, the key features of BrS. Slope factors for inactivation were comparable (WT, 6.93 ± 0.23 mV; E1784K, 7.09 ± 0.12 mV), but slope factors of activation were significantly larger in E1784K (WT, –6.08 ± 0.26 mV; E1784K, –8.06 ± 0.20 mV; $P < 0.001$), indicating that the activation in E1784K was less voltage sensitive (Figure 4A).

The proportion of channels available depends on the extent of recovery from inactivation. Recovery from fast inactivation was assessed by a standard double-pulse protocol using a recovery potential of –120 mV, and there was no difference between WT and E1784K in the time constants for inactivation and the fractions of fast or slow recovery components (Figure 4B). Some mutant Na channels, including 1795insD (10) and T1620M (20), have been reported to display defects in the kinetics of or recovery from a "slower" inactivation process, sometimes referred to as I_M, and this defect is recognized as an important biophysical feature in some cases of BrS (21). This may explain the greater reduction in Na channel availability during excitation in LQT3 patients with 1795insD (10) compared with those with ΔKPQ. We therefore analyzed the onset of I_M by varying prepulses of 1 ms to 2 s followed by a brief hyperpolarization to allow channels to recover from fast inactivation prior to a final test pulse. Double exponential curve fitting revealed that the amplitude of the fraction of the fast inactivating component (A_f) was significantly larger in E1784K (WT, 0.12 ± 0.02, $n = 10$; E1784K, 0.20 ± 0.02, $n = 12$; $P < 0.005$), and τ_f was significantly smaller in E1784K (WT, 1883 ± 669 ms; E1784K, 554 ± 101 ms; $P < 0.05$). Other parameters were comparable between WT and E1784K; (A_s: WT, 0.24 ± 0.04; E1784K, 0.19 ± 0.01; P = NS; τ_f: WT, 6.6 ± 3.5 ms; E1784K, 1.3 ± 0.2; P = NS; constant value A_c: WT, 0.64 ± 0.04; E1784K, 0.60 ± 0.01; P = NS). These data show that the extent of I_M was significantly enhanced in E1784K similar to 1795insD (10), and provide a further mechanism for the reduced channel availability.

Another possible pathophysiological mechanism underlying the reduced peak Na current responsible for Brugada-type ST elevation in LQT3 is failure of mutant channel proteins to be properly trafficked to the cell surface (22, 23). To test this concept, an extracellular FLAG epitope was introduced in both WT and E1784K channels, and their cellular distribution was determined by a confocal laser scanning microscopy in tsA-201cells. As depicted in the *xz* and *yz* sections of Figure 4D, the distributions of anti-FLAG antibody were predominantly expressed in the plasma membrane and indistinguishable between WT and E1784K with or without coexpression of β1 subunit (that has been implicated

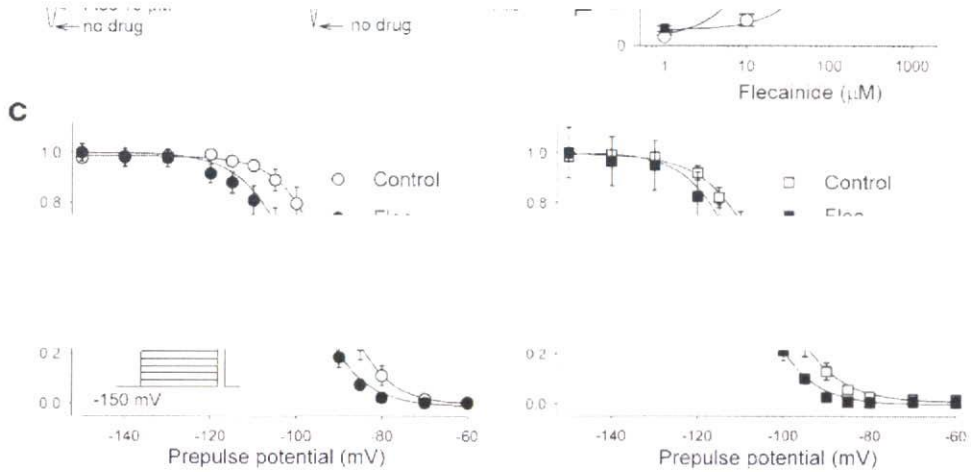

Figure 6

State-dependent flecainide block. (**A**) Representative steady-state current traces of WT and E1784K before and after flecainide (10 and 100 μmol/l). Cells were depolarized by –20 mV from a holding potential of –150 mV. Currents were normalized by the peak current before flecainide and were superimposed. Calibration bars indicate 1 nA and 1 ms. (**B**) Concentration-response curve for flecainide-induced tonic block in WT (n = 5) and E1784K (n = 5). The normalized peak currents were fit to the Hill equation $B(\%) = 100/(1 + (D / IC_{50})^{nH})$, where B is the percentage block at drug concentration D, and nH is the Hill coefficient. The IC_{50} values, representing dissociation constants for resting state (K_R) were WT, 150.3 μmol/l and E1784K, 20.4 μmol/l. Thus the mutant channel was far more sensitive to tonic block by flecainide. (**C**) Dissociation constant for inactivated channels. Cells were depolarized by prepulses ranging from –150 mV to –60 mV for 500 ms from a holding potential of –150 mV to ensure steady-state inactivation, followed by a –20-mV test pulse in the presence or absence of 30 μmol/l flecainide. The pulse protocol cycle time was 60 s. Peak Na currents were normalized to the maximum Na current in the absence or presence of flecainide and were fit to the Boltzmann equation. The dissociation constant for the inactivated state (K_I) was calculated using Bean's equation (27): $V_{1/2} - V_{1/2c} = k \times ln([1 + D / K_R] / [1 + D / K_I])$, where $V_{1/2}$ and $V_{1/2c}$ are the midpoints of steady-state inactivation for flecainide and control, respectively, D is the flecainide concentration, and K_R is the dissociation constant for the resting state. The K_R values are equivalent to the IC_{50} values measured at a holding potential of –150 mV (WT, 150.3 μmol/l; E1784K, 20.4 μmol/l) in **B**.

as a modulator of cell surface expression; ref. 24). Figure 4E shows the quantitative analysis of the fluorescent intensity in the membrane divided by the fluorescence intensity of entire cell area measured from 10 to 13 cells. Fluorescence intensity in the membrane was comparable between WT and E1784K regardless of the coexpressed β1 subunit (WT, 71.5 ± 3.5%, n = 12; E1784K, 72.9 ± 2.0%, n = 10; WT + β1, 71.1 ± 2.2%, n = 13; E1784K + β1, 68.4 ± 1.6%, n = 12; P = NS). Thus our immunocytochemical analyses provide strong evidence that the loss-of-function properties displayed by E1784K are most likely attributable to the observed changes in current gating rather than a change in channel density.

Molecular mechanisms of enhanced flecainide sensitivity. Class IC Na channel blockers generated the BrS phenotype in 5 of 9 patients challenged. We therefore investigated tonic block and use-dependent block (UDB) by flecainide in WT and E1784K channels expressed in tsA-201 cells, and compared them with those of T1304M, a mutation that did not show ST elevation during the flecainide challenge test (13). Cells transfected with WT, E1784K, or T1304M were depolarized by 2-Hz pulse trains at –20 mV for 20 ms from the holding potential of –120 mV in the absence or presence of 10 μmol/l flecainide. Under drug-free conditions, peak current reduction after the 100 pulses was less than 2% of the peak current for WT, E1784K, and T1304M. During exposure to 10 μmol/l flecainide, peak currents normalized to predrug baseline were progressively reduced by the repetitive pulses (Figure 5, A and B). There was a remarkable difference in the extent of first pulse (tonic) block that was only 4.5% ± 4.0% for WT (n = 5), and 7.1% ± 2.7% for T1304M (n = 5, P = NS), compared with substantial tonic block in E1784K (43.7% ± 8.0%, n = 5, P < 0.001). Conversely, UDB, determined by the difference in peak current values between the first and hundredth test pulses relative to the first pulse, was slightly attenuated in E1784K (WT, 43.4% ± 3.0%; E1784K, 32.0% ± 2.2%; P < 0.05), but not in T1304M (36.9% ± 2.7%; P = NS) (Figure 5C). The net effect of flecainide after a train of 100 pulses was significantly greater in E1784K than WT (WT, 45.5% ± 5.0%; E1784K, 61.8% ± 2.5%; P < 0.001) but not in T1304M (41.2% ± 3.2%; P = NS). This attenuated flecainide UDB in E1784K is in striking contrast to that reported for 1795insD (12) and ΔKPQ (25), which showed enhancement in both tonic and use-dependent flecainide block. UDB is profoundly affected by the recovery from drug block, and delayed recovery from flecainide block has been

Table 1
Reported biophysical properties of LQT3 mutations

	SCN5A mutations				
	1795insD	**ΔKPQ**	**ΔK1500**	**E1784K**	**T1304M**
Clinical features					
QT prolongation	+	+	+	+	+
ST elevation[A]	+	+	+	+	–
Sinus node dysfunction	+	+	+	+	–
Biophysical and pharmacological properties					
Persistent Na current	+	+	+	+	+
Shift of $V_{1/2}$ (inactivation)	Negative	Negative	Negative	Negative	Positive
Shift of $V_{1/2}$ (activation)	Positive	Positive	Positive	Positive	Positive
Current decay	Slower	Faster	↔	Faster	Faster
Recovery from inactivation	Slower	Faster	ND	↔	Faster
Slow inactivation	Enhanced	↔	ND	Enhanced	↔
Tonic block by flecainide	Enhanced	Enhanced	Enhanced	Enhanced	↔
UDB by flecainide	Enhanced	Enhanced	ND	Diminished	↔
References	10, 11, 28	2, 25, this study	15	17, this study	29, this study

[A]Spontaneous or Na channel blocker–induced ST elevation. ↔, comparable with WT; ND, not determined.

implicated in the augmented flecainide sensitivity in 1795insD (12) and ΔKPQ (25). Accordingly, we evaluated recovery from flecainide block using the protocol shown in the inset of Figure 5D. Cells were initially subjected to 50 pulses (–20 mV for 20 ms) from a holding potential of –150 mV at 10 Hz in the presence of 30 μmol/l flecainide, followed by a variable recovery time (Δt) and a test pulse of –20 mV. Recovery from flecainide block was virtually identical among all 3 channels, compatible with the observation that the drug-free recovery from inactivation of WT and E1784K were comparable (Figure 4B). Taken together, these results indicate that the E1784K channels are much more sensitive to block by flecainide than are the WT and T1304M channels, and that this augmented sensitivity is attributable to enhanced tonic block rather than a change in UDB.

If the extent of tonic block roughly parallels the voltage dependence of availability of drug-free channels, then the difference between WT and E1784K should be attenuated when cells are depolarized from a very negative holding potential, where the channels will be similarly available (Figure 4A). At a holding potential of –150 mV, the magnitude of flecainide tonic block was diminished in both WT and E1784K, but tonic block at –150 mV was still greater in E1784K (Figure 6A). Dose-response curves for flecainide block measured at a holding potential of –150 mV (thus representing drug affinity for the resting state) are shown in Figure 6B. The E1784K channels were 7.5-fold more sensitive to resting-state block by flecainide than were the WT channels (IC_{50}: WT, 150.3 μmol/l; E1784K, 20.4 μmol/l).

The diminished UDB in E1784K may be attributable to reduced flecainide affinity for inactivated channels. To test this idea, flecainide affinity for the inactivated state was measured as previously described (26). Steady-state channel availability was determined in the presence or absence of 30 μmol/l flecainide by using 500 ms prepulses ranging from –150 to –60 mV to ensure a steady state before the test pulse (Figure 6C). The apparent dissociation constant for the inactivated channels (K_I) was calculated using Bean's equation (27). K_I values for flecainide of WT and E1784K were comparable (WT, 7.1 μmol/l; E1784K, 5.4 μmol/l). These results suggest that the enhanced sensitivity to flecainide of the E1784K is explained mainly by gating-dependent mechanisms of the mutant channel (i.e., enhanced inactivation), but increased drug affinity to resting-state channels may also be involved.

Spectrum of SCN5A dysfunction in LQT3 associated with BrS and sinus node dysfunction. There are several possible loss-of-function properties of the Na channel that have been linked to the BrS phenotype. These include a negative shift of steady-state inactivation (which includes enhanced closed-state inactivation) (12), a positive shift of activation, faster current decay, enhanced slow inactivation (20), slower recovery from inactivation, a trafficking defect of the channel molecule (22), and enhanced sensitivity to Na channel blockers.

To explore the functional determinants for the phenotypic overlap of BrS in LQT3 patients, we compared the biophysical and pharmacological properties of reported LQT3 mutations and sought features commonly and specifically observed in those manifesting a BrS phenotype (Table 1). The overlapping phenotype (LQT3 and BrS) has been previously reported for 1795insD (10, 11), ΔKPQ (13, 14), ΔK1500 (15), and E1784K (13). In contrast, a carrier of T1304M did not show ST elevation during a flecainide test (13). Similarly, sinus node dysfunction has been reported in carriers of the same *SCN5A* mutations, 1795insD (28), ΔKPQ (16), ΔK1500 (15), E1784K (17), and D1790G (7), but not in other *SCN5A* mutations, including T1304M. Thus, it is plausible to speculate that the biophysical characteristics common to these mutations but not found in T1304M are channel properties responsible for evoking mixed phenotypes of BrS and sinus node dysfunction in patients with LQT3. To this end, Table 1 compares the functional properties of E1784K and those reported for 1795insD, ΔKPQ, ΔK1500, E1784K, and T1304M (29). Because inconsistency with the gating properties of ΔKPQ has been noted among several reports, we reevaluated this mutant under conditions identical to those we used for E1784K. Consistent with the initial report by Bennett et al. (2), steady-state inactivation of ΔKPQ was significantly shifted in the negative direction by –8.9 mV ($V_{1/2}$ = –95.7 ± 1.1 mV, n = 7) compared with WT, and activation was significantly shifted in the positive direction ($V_{1/2}$ = –34.9 ± 0.9 mV, n = 7), similar to E1784K. Among the biophysical properties listed in Table 1, we found that both the negative shift in steady-state inactivation and

the enhanced tonic block by flecainide are common to 1795insD, ΔKPQ, ΔK1500, and E1784K, but not to T1304M. This negative shift of inactivation will reduce the availability of the channels at the resting membrane potential and increase the proportion of inactivated channels in both the open and closed states, reducing Na current and increasing the sensitivity to Na channel blockers. A positive shift in activation is another loss-of-function property evident in all the mutants including T1304M, making it less likely that this specific channel property underlies mixed clinical phenotypes in LQT3. Other channel properties such as current decay, recovery from inactivation, slow inactivation, or UDB were not common among 1795insD, ΔKPQ, ΔK1500, and E1784K.

Discussion

The main findings of this study are that the *SCN5A* mutation, E1784K, was found in 34% of LQT3 probands and showed overlapping clinical phenotypes of BrS and sinus node dysfunction in patients from different genetic backgrounds. In vitro functional characterization of this mutation and comparison to properties reported for other LQT3 variants suggest that a negative shift of steady-state Na channel inactivation and enhanced tonic block in response to Na channel blockers confer an additional BrS/sinus node dysfunction phenotype.

E1784K was originally reported by Wei et al. (17) and subsequently by several other groups (13, 30–32). Other groups have also indicated that this is a common LQT3 mutation. Napolitano et al. previously reported that E1784K is a "non-private" LQT3 mutation (i.e., that it occurred more than once in their LQTS population) (33). Similarly, in genetic screening of 541 unrelated LQTS patients, Tester et al. demonstrated that E1784K was the most prevalent LQT3 mutation (4/26, 15.4%) (32).

Na channel blocker therapy is widely used in LQT3 because of block of persistent Na current during repolarization (34). However, these agents, especially class IC drugs, also unmask or exacerbate ST elevation in BrS. Despite this apparent divergence of Na channel blocker action, some LQT3 patients display ST elevation characteristic of BrS spontaneously (10–12) or during class IC drug therapy (13, 14). The results of the present study indicate that the BrS/LQT3 overlap is not likely to reflect coinherited genetic variations, gender, or ethnicity and thus implicate the biophysical properties of specific mutant channels as the primary mediator of this mixed phenotype. Furthermore, this overlapping phenotype appears to be more common than generally recognized because it is observed in E1784K (a prevalent mutation), as well as other LQT3 mutations (1795insD, ΔKPQ, ΔK1500). These observations have raised a concern about the safety of class IC drug therapy in LQT3 patients (13) and prompted us to examine in more detail the underlying mechanisms of drug-induced block in Na channels with these mutations.

The mutation 1795insD (10–12), which produces an overlapping phenotype, generates a wide range of biophysical abnormalities, including a negative shift in inactivation, enhanced slow inactivation, and delayed recovery from inactivation in addition to the hallmark LQT3 abnormality of non-inactivating persistent Na current (12). This negative shift of steady-state inactivation, which is compatible with enhanced closed-state inactivation, tends to increase the proportion of the inactivated channels at the resting potential and thus augments tonic block by flecainide. This property, as well as increased persistent current, is commonly observed in the 3 other LQT3 mutations associated with BrS and sinus node dysfunction (E1784K, ΔKPQ, and ΔK1500). However, T1304M, which is not associated with BrS or sinus node dysfunction, shows a positive shift of steady-state inactivation (Table 1).

Enhanced slow inactivation and UDB, which are thought to underlie the phenotype produced by T1620M (20), a "BrS-only" (non-LQT3) mutation, have also been reported with 1795insD (12). Although slow inactivation was enhanced in E1784K (Figure 4C), and UDB was enhanced in ΔKPQ (25), these characteristics are not common among the 4 mutations with LQT3/BrS overlap. Indeed, UDB by flecainide was diminished in E1784K (Figure 5, A–C). These findings suggest that slow inactivation or use-dependent inactivation is not the principal mechanism for the BrS-type ST elevation in LQT3.

In addition to right precordial ST elevation, a secondary phenotype of sinus node dysfunction has been reported in 4 *SCN5A* mutations (E1784K, 1795insD, ΔKPQ, and ΔK1500). Although the functional relevance of Na channels in sinus nodal pacemaker function has been debated, there is evidence for Na current in the sinus node periphery (35), and other TTX-sensitive Na channels may contribute (36). Patch clamp and computer simulation studies of 1795insD have demonstrated that the negative shift of inactivation reduces Na current during diastolic depolarization; also, the persistent Na current increases action potential duration, leading to a slowing of sinus rate (28). A negative shift in inactivation is observed in E1784K, 1795insD, ΔKPQ, and ΔK1500 and may play a role in the overlap of the LQT3 clinical phenotype with BrS and sinus node dysfunction in the mutation carriers. In summary, a negative shift in inactivation and enhanced tonic block are common biophysical properties observed among *SCN5A* mutations with the LQT3/BrS overlapping phenotype. These findings suggest that prophylactic class IC drugs should be avoided in LQT3 mutations displaying these biophysical properties in vitro.

Because this was a multicenter study, the Na channel blockers used for provocation testing were not the same. In addition, 4 patients challenged with flecainide did not display right precordial ST elevation; this negative flecainide test in 1 individual could have been due to variable efficacy of Na channel blockers or day-to-day variability in autonomic tone (37). While a negative shift in steady-state inactivation appears to be a common biophysical property among LQT3 mutations (including E1784K) displaying the mixed phenotype, the number of LQT3 mutations that have been evaluated in this detail is still small. Moreover, biophysical and pharmacological properties presented in tsA-201 cells may not necessarily reflect the situation in vivo, and the effects of the mutation may be different in ventricular myocytes compared with sinus node cells. Thus, further studies that combine clinical and in vitro phenotyping in LQT3 mutations with and without overlapping clinical phenotypes will be required to confirm the findings of the present study.

E1784K is the most common LQT3 mutation. In patients with this and other LQT3 mutations, overlap with BrS and sinus node dysfunction is relatively common. Our in vitro studies with E1784K and previous reports in LQT3 mutations with and without this clinical overlap syndrome implicate a negative shift in inactivation and enhanced tonic block by drugs as underlying mechanisms. These data suggest that patients with LQT3 mutations displaying these characteristics in vitro should not receive class IC drugs. Furthermore, the present findings reinforce the general concept that in vitro characterization of the function of ion channel variants is a key component in generating specific therapeutic strategies for patient management.

Methods

Clinical evaluation

The study population included 44 genotyped LQT3 families with different ethnic backgrounds (20 Asian, 24 Caucasian) ascertained from a total of 7 institutions (Japan, n = 3; USA, England, Italy, and Germany, n = 1 each). In these families, E1784K (c. 5350C→A) was the most prevalent *SCN5A* mutation (n = 15; 34%). The mean age of the probands (10 men, 5 women) was 22 ± 11 years at diagnosis (mean ± SD, ranging from 7 to 43 years). Two probands died suddenly (A:II:6 and C:III:1; Figure 1), one at rest and the other whilst driving a car. In both cases, no ante mortem data was available and an autopsy could not establish a cause of death. The 15 families were comprised of 93 surviving members, of whom 66 underwent genetic testing. Family members underwent physical examination, ECG, exercise stress test, and Holter recording. The diagnosis of LQTS in the probands, or in the family members if probands died suddenly before evaluation, was established using the revised criteria suggested by Schwartz (8). Na channel blocker challenge was conducted using mexiletine (2 mg/kg), flecainide (2 mg/kg), ajmaline (1 mg/kg), or pilsicainide (1 mg/kg) administered intravenously, with positive (coved) and negative responses determined using standard 12-lead ECGs, as previously described (38).

Sinus node dysfunction was considered if one of the following conditions was recorded at one or more occasions when inappropriate for the circumstances: (a) sinus bradycardia, (b) sinus arrest or exit block, and (c) combinations of sinoatrial and atrioventricular conduction disturbances; these bradyarrhythmias often occurred in conjunction with paroxysmal atrial tachyarrhythmias (39).

Genetic analysis

All probands and family members who participated in the study gave written informed consent before the genetic and clinical investigations, in accordance with the standards of the Declaration of Helsinki and local ethics committees. Genetic analysis was performed on genomic DNA extracted from peripheral white blood cells using standards methods. Coding regions of *KCNQ1*, *KCNH2*, *SCN5A*, *KCNE1*, and *KCNE2* were amplified by PCR using exon-flanking intronic primers (31, 40), and direct DNA sequencing was performed using ABI 310, 3130, and 3730 genetic analyzers (Applied Biosystems) (17). In some cases, denaturing high-performance liquid chromatography with the Transgenomic Wave Instrument (Transgenomic Inc.) was applied for the screening of polymorphisms prior to direct sequencing.

Construction of expression plasmids and transfection of mammalian cell lines. A 0.5-kb HindIII/XhoI fragment (5′ cloning site – nt. 533) and a 1.6-kb BstEII/XbaI fragment (nt. 4626 – 3′ cloning site) of WT human heart Na channel α subunit (Nav1.5) were subcloned into the pBluescript II SK+ plasmid (Stratagene) for the mutagenesis to generate the FLAG-tagged channel and E1784K, respectively. Site-directed mutagenesis was performed by QuikChange site-directed mutagenesis kit (Stratagene) according to the manufacturer's instructions. A FLAG-tagged Nav1.5 plasmid was constructed by inserting the FLAG (DYKDDDK) epitope in frame at the extracellular loop of the domain 1 between Pro154 and Pro155. The FLAG-tag did not change the current densities or the gating properties of Nav1.5 (data not shown). Final constructs were assembled in the mammalian expression plasmid pcDNA3.1+ (Invitrogen) and then sequenced to verify creation of mutation and exclude polymerase errors. The plasmids encoding ΔKPQ and T1304M were constructed as previously described (2, 29). The human cell line tsA-201 was transiently transfected with WT, E1784K ΔKPQ, or T1304M plasmid using Lipofectamine (Invitrogen) or SuperFect (Qiagen) in combination with a bicistronic plasmid (pCD8-IRES-hβ$_1$) encoding CD8 and the human Na channel β$_1$ subunit (hβ$_1$) to visually identify cells expressing heterologous hβ$_1$ with Dynabeads M-450 CD8 (Dynal) (41). Electrophysiological measurements were performed 24–72 h after transfection.

Electrophysiology and data analysis. Na currents were recorded using the whole-cell patch clamp technique as previously described (41). Electrode resistance ranged from 0.8 to 1.5 MΩ. Data acquisition was carried out using an Axopatch 200B patch clamp amplifier and pCLAMP8 software (Axon Instruments). Currents were filtered at 5 kHz (–3 dB; 4-pole Bessel filter) and digitized using an analog-to-digital interface (Digidata 1322A; Axon Instruments). Experiments were carried out at room temperature (20–22°C). Voltage errors were minimized using series resistance compensation (generally 80%). Cancellation of the capacitance transients and leak subtraction were performed using an online P/4 protocol. The pulse protocol cycle time was 10 s unless otherwise stated. The data were analyzed using Clampfit 10 (Axon Instruments) and SigmaPlot 9 (SPSS Science). The holding potential was –120 mV unless otherwise stated. The bath solution contained (in mmol/l): 145 NaCl, 4 KCl, 1.8 $CaCl_2$, 1 $MgCl_2$, 10 HEPES, and 10 glucose, pH 7.35 (adjusted with NaOH). The pipette solution (intracellular solution) contained (in mmol/l): 10 NaF, 110 CsF, 20 CsCl, 10 EGTA, and 10 HEPES, pH 7.35 (adjusted with CsOH). The time from establishing the whole-cell configuration to onset of recording was consistent cell-to-cell to exclude the possible time-dependent shift of steady-state inactivation.

To determine activation parameters, the current-voltage relationship was fit to the Boltzmann equation $I = (V - V_{rev}) \times G_{max} \times (1 + \exp[V - V_{1/2}] / k)^{-1}$, where I is the peak Na current during the test pulse potential V. The parameters estimated by the fitting are V_{rev} (reversal potential), G_{max} (maximum conductance), and k (slope factor). Steady-state availability for fast inactivation was measured with a standard double-pulse protocol (Figure 4A, inset), and the data were fit with the Boltzmann equation $I/I_{max} = (1 + \exp[(V - V_{1/2}) / k])^{-1}$, where I_{max} is the maximum peak Na current, to determine the membrane potential for $V_{1/2}$ and k. Macroscopic current decay was analyzed by fitting data with a double exponential equation: $I/I_{max} = A_\infty + A_f \times \exp(-t/\tau_f) + A_s \times \exp(-t/\tau_s)$, where A_∞ and t are constant value and time, respectively; A_f and A_s are fractions of fast and slow inactivating components, respectively; and τ_f and τ_s are time constants of A_f and A_s, respectively. Recovery from inactivation was assessed by the double-pulse protocol (Figure 4B, inset) and was analyzed by fitting the data to a double exponential equation: $I/I_{max} = A_\infty + A_f \times \exp(-t/\tau_f) + A_s \times \exp(-t/\tau_s)$. The onset of slow inactivation was measured by the double-pulse protocol shown in the inset of Figure 4C. A brief repolarization pulse was applied to allow most channels to recover from fast inactivation, and the data were fit with biexponential functions.

In some experiments, cells were superfused with bath solution containing flecainide or TTX to determine their pharmacological effects. During the superfusion, cells were held at –120 mV unless otherwise stated. Tonic block was defined as a diminution in the peak Na current of the first depolarizing pulse after the exposure to the drug compared with that in the control, and UDB as a diminution in the peak Na current of the hundredth pulse compared with that of the first pulse after the drug. Flecainide (acetate salt) was made up in a 10 mmol/l stock solution and diluted in a bath solution, and data were recorded after 3-min periods for drug equilibration. All the chemicals were purchased from Sigma-Aldrich or Wako, except for flecainide and mexiletine, which were gifts from Eisai and Nippon Boehringer Ingelheim, respectively.

Immunocytochemistry. TsA-201 cells were transfected with the pcDNA3.1+Nav1.5 plasmid encoding either WT or E1784K together with or without pCD8-IRES-hβ1. Two days later, cells were incubated with Dynabeads M-450 CD8 (Dynal) for 30 min at 37°C to identify the cells expressing both hβ1 and CD8. The cells were then washed with PBS (pH 7.4), fixed in PBS containing 2% formaldehyde for 30 min at 4°C, and

permeabilized with 0.05% Triton X-100 for 30 min at 4°C. After blocking with PBS containing 4% BSA for 1 h at room temperature, the cells were stained with anti-FLAG M2 monoclonal antibody (Sigma-Aldrich) for 1 h at room temperature. Protein reacting with antibody was visualized with Alexa Fluor 488–labeled secondary antibody (Molecular Probes). Optical sections of Alexa Fluor 488 were obtained with a FluoView FV1000 confocal laser scanning microscope (Olympus Corp.) with a ×60 oil immersion objective lens. To quantify the membrane expression of Nav1.5, fluorescence intensity at the entire cell area and the plasma membrane region in the middle *xy* image of *z* series stack was measured using MetaMorph 6.1 software (Molecular Devices).

Statistics. Results are presented as means ± SEM unless otherwise stated, and statistical comparisons were made using ANOVA with the Dunnett post-hoc test to evaluate the significance of differences between means. Statistical significance was assumed for $P < 0.05$.

Acknowledgments

This work was supported in part by grants from MEXT Japan (18590757 to N. Makita and 14370225, 16209025, and 19390212 to M. Horie); the Ministry of Health, Labour and Welfare, Japan (H18-Research on Human Genome-002 to N. Makita, W. Shimizu, and M. Horie; Research on Nanotechnical Medical, H19-nano-006 to N. Mochizuki); the Uehara Memorial Foundation (to W. Shimizu); the Program for the Promotion of Fundamental Studies in Health Sciences of the National Institute of Biomedical Innovation (to N. Mochizuki); the US Public Health Service (HL49989 and HL46681 to D.M. Roden, HL65962 to A.L. George Jr. and D.M. Roden, and HL33843 to L. Crotti and P.J. Schwartz); the Collaborative Research Effort (SFB, project C1) of the DFG (to E. Schulze-Bahr); the DFG (DFG Schu1082/3-1 and 3-2 to E. Schulze-Bahr); and the Fondation Leducq (to E. Schulze-Bahr). We thank M. Fukuoka, K. Kawai, and N. Ohashi for technical assistance.

Received for publication September 25, 2007, and accepted in revised form February 27, 2008.

Address correspondence to: Naomasa Makita, Department of Cardiovascular Medicine, Hokkaido University Graduate School of Medicine, Kita-15, Nishi-7, Kita-Ku, Sapporo 060-8638, Japan. Phone: 81-11-706-6973; Fax: 81-11-706-7874; E-mail: makitan03@ybb.ne.jp.

1. Keating, M.T. 1996. The long QT syndrome. A review of recent molecular genetic and physiologic discoveries. *Medicine.* **75**:1–5.
2. Bennett, P.B., Yazawa, K., Makita, N., and George, A.L., Jr. 1995. Molecular mechanism for an inherited cardiac arrhythmia. *Nature.* **376**:683–685.
3. Chen, Q., et al. 1998. Genetic basis and molecular mechanism for idiopathic ventricular fibrillation. *Nature.* **392**:293–296.
4. Schott, J.J., et al. 1999. Cardiac conduction defects associate with mutations in SCN5A. *Nat. Genet.* **23**:20–21.
5. Benson, D.W., et al. 2003. Congenital sick sinus syndrome caused by recessive mutations in the cardiac sodium channel gene (SCN5A). *J. Clin. Invest.* **112**:1019–1028.
6. Schwartz, P.J., et al. 1995. Long QT syndrome patients with mutations of the SCN5A and HERG genes have differential responses to Na^+ channel blockade and to increases in heart rate. Implications for gene-specific therapy. *Circulation.* **92**:3381–3386.
7. Benhorin, J., et al. 2000. Effects of flecainide in patients with new SCN5A mutation: Mutation-specific therapy for long-QT syndrome? *Circulation.* **101**:1698–1706.
8. Schwartz, P.J. 2006. The congenital long QT syndromes from genotype to phenotype: clinical implications. *J. Intern. Med.* **259**:39–47.
9. Antzelevitch, C. 2001. The Brugada syndrome: ionic basis and arrhythmia mechanisms. *J. Cardiovasc. Electrophysiol.* **12**:268–272.
10. Veldkamp, M.W., et al. 2000. Two distinct congenital arrhythmias evoked by a multidysfunctional Na^+ channel. *Circ. Res.* **86**:E91–E97.
11. Bezzina, C., et al. 1999. A single Na^+ channel mutation causing both long-QT and Brugada syndromes. *Circ. Res.* **85**:1206–1213.
12. Viswanathan, P.C., et al. 2001. Gating-dependent mechanisms for flecainide action in SCN5A-linked arrhythmia syndromes. *Circulation.* **104**:1200–1205.
13. Priori, S.G., et al. 2000. The elusive link between LQT3 and Brugada syndrome: The role of flecainide challenge. *Circulation.* **102**:945–947.
14. Moss, A.J., et al. 2005. Safety and efficacy of flecainide in subjects with long QT-3 syndrome (ΔKPQ Mutation): A randomized, double-blind, placebo-controlled clinical trial. *Ann. Noninvasive Electrocardiol.* **10**:59–66.
15. Grant, A.O., et al. 2002. Long QT syndrome, Brugada syndrome, and conduction system disease are linked to a single sodium channel mutation. *J. Clin. Invest.* **110**:1201–1209.
16. Moss, A.J., et al. 1995. ECG T-wave patterns in genetically distinct forms of the hereditary long QT syndrome. *Circulation.* **92**:2929–2934.
17. Wei, J., et al. 1999. Congenital long-QT syndrome caused by a novel mutation in a conserved acidic domain of the cardiac Na^+ channel. *Circulation.* **99**:3165–3171.
18. Berg, M.P., et al. 2001. Possible bradycardic mode of death and successful pacemaker treatment in a large family with features of long QT syndrome type 3 and Brugada syndrome. *J. Cardiovasc. Electrophysiol.* **12**:630–636.
19. Schwartz, P. 1980. The long QT syndrome. In *Sudden death.* H. Kulbertus and H. Wellens, editors. Springer-Verlag. New York, New York, USA. 358–378.
20. Wang, D.W., Makita, N., Kitabatake, A., Balser, J.R., and George, A.L., Jr. 2000. Enhanced Na^+ channel intermediate inactivation in Brugada syndrome. *Circ. Res.* **87**:E37–E43.
21. Balser, J.R. 2001. The cardiac sodium channel: gating function and molecular pharmacology. *J. Mol. Cell. Cardiol.* **33**:599–613.
22. Baroudi, G., et al. 2001. Novel mechanism for Brugada syndrome: Defective surface localization of an *SCN5A* mutant (R1432G). *Circ. Res.* **88**:e78–e83.
23. Liu, K., Yang, T., Viswanathan, P.C., and Roden, D.M. 2005. New mechanism contributing to drug-induced arrhythmia: rescue of a misprocessed LQT3 mutant. *Circulation.* **112**:3239–3246.
24. Isom, L.L., et al. 1995. Functional co-expression of the β1 and type IIA α subunits of sodium channels in a mammalian cell line. *J. Biol. Chem.* **270**:3306–3312.
25. Nagatomo, T., January, C.T., and Makielski, J.C. 2000. Preferential block of late sodium current in the LQT3 Delta KPQ mutant by the class IC antiarrhythmic flecainide. *Mol. Pharmacol.* **57**:101–107.
26. Sasaki, K., et al. 2004. Unexpected mexiletine responses of a mutant cardiac Na^+ channel implicate the selectivity filter as a structural determinant of antiarrhythmic drug access. *Mol. Pharmacol.* **66**:330–336.
27. Bean, B., Cohen, C., and Tsien, R. 1983. Lidocaine block of cardiac sodium channels. *J. Gen. Physiol.* **81**:613–642.
28. Veldkamp, M.W., et al. 2003. Contribution of sodium channel mutations to bradycardia and sinus node dysfunction in LQT3 families. *Circ. Res.* **92**:976–983.
29. Wang, D.W., et al. 2007. Cardiac sodium channel dysfunction in sudden infant death syndrome. *Circulation.* **115**:368–376.
30. Deschenes, I., et al. 2000. Electrophysiological characterization of SCN5A mutations causing long QT (E1784K) and Brugada (R1512W and R1432G) syndromes. *Cardiovasc. Res.* **46**:55–65.
31. Splawski, I., et al. 2000. Spectrum of mutations in long-QT syndrome genes. KVLQT1, HERG, SCN5A, KCNE1, and KCNE2. *Circulation.* **102**:1178–1185.
32. Tester, D.J., Will, M.L., Haglund, C.M., and Ackerman, M.J. 2005. Compendium of cardiac channel mutations in 541 consecutive unrelated patients referred for long QT syndrome genetic testing. *Heart Rhythm.* **2**:507–517.
33. Napolitano, C., et al. 2005. Genetic testing in the long QT syndrome: Development and validation of an efficient approach to genotyping in clinical practice. *JAMA.* **294**:2975–2980.
34. Kambouris, N.G., et al. 2000. A revised view of cardiac sodium channel "blockade" in the long-QT syndrome. *J. Clin. Invest.* **105**:1133–1140.
35. Tellez, J.O., et al. 2006. Differential expression of ion channel transcripts in atrial muscle and sinoatrial node in rabbit. *Circ. Res.* **99**:1384–1393.
36. Maier, S.K.G., et al. 2003. An unexpected requirement for brain-type sodium channels for control of heart rate in the mouse sinoatrial node. *Proc. Natl. Acad. Sci. U. S. A.* **100**:3507–3512.
37. Miyazaki, T., et al. 1996. Autonomic and antiarrhythmic drug modulation of ST segment elevation in patients with Brugada syndrome. *J. Am. Coll. Cardiol.* **27**:1061–1070.
38. Brugada, R., et al. 2000. Sodium channel blockers identify risk for sudden death in patients with ST-segment elevation and right bundle branch block but structurally normal hearts. *Circulation.* **101**:510–515.
39. Olgin, J.E., and Zipes, D.P. 2001. Specific arrhythmias: diagnosis and treatment. In *Heart disease: a textbook of cardiovascular medicine.* E. Braunwald, D.P. Zipes, and P. Libby, editors. W.B. Saunders. Philadelphia, Pennsylvania, USA. 815–899.
40. Wang, Q., Li, Z., Shen, J., and Keating, M.T. 1996. Genomic organization of the human SCN5A gene encoding the cardiac sodium channel. *Genomics.* **34**:9–16.
41. Makita, N., et al. 2002. Drug-induced long-QT syndrome associated with a subclinical SCN5A mutation. *Circulation.* **106**:1269–1274.

Age- and Genotype-Specific Triggers for Life-Threatening Arrhythmia in the Genotyped Long QT Syndrome

TOMOKO SAKAGUCHI, M.D.,* WATARU SHIMIZU, M.D., PH.D.,†
HIDEKI ITOH, M.D., PH.D.,* TAKASHI NODA, M.D., PH.D.,†
YOSHIHIRO MIYAMOTO, M.D., PH.D.,‡ IORI NAGAOKA, M.D.,* YUKO OKA, M.D.,*
TAKASHI ASHIHARA, M.D., PH.D.,* MAKOTO ITO, M.D., PH.D.,* KEIKO TSUJI, M.S.,*
SEIKO OHNO, M.D., PH.D.,§ TAKERU MAKIYAMA, M.D., PH.D.,§
SHIRO KAMAKURA, M.D., PH.D.,† and MINORU HORIE, M.D., PH.D.*

From the *Department of Cardiovascular Medicine, Shiga University of Medical Science, Otsu, Japan; †Division of Cardiology, Department of Internal Medicine, National Cardiovascular Center, Suita, Japan; ‡Laboratory of Molecular Genetics, National Cardiovascular Center, Suita, Japan; and §Department of Cardiovascular Medicine, Kyoto University Graduate School of Medicine, Kyoto, Japan

Age and Long QT Syndrome. ***Introduction:*** **Patients with long QT syndrome (LQTS) become symptomatic in adolescence, but some become at age of ≥20 years. Since it remains unknown whether clinical features of symptomatic LQTS patients differ depending on the age of onset, we aimed to examine whether triggers for cardiac events are different depending on the age in genotyped and symptomatic LQTS patients.**

Methods and Results: **We identified 145 symptomatic LQTS patients, divided them into three groups according to the age of first onset of symptoms (young <20, intermediate 20–39, and older ≥40 years), and analyzed triggers of cardiac events (ventricular tachycardia, syncope, or cardiac arrest). The triggers were divided into three categories: (1) adrenergically mediated triggers: exercise, emotional stress, loud noise, and arousal; (2) vagally mediated triggers: rest/sleep; and (3) secondary triggers: drugs, hypokalemia, and atrioventricular (AV) block. In the young group, 78% of the cardiac events were initiated by adrenergically mediated triggers and 22% were vagally mediated, but none by secondary triggers. In contrast, the adrenergically mediated triggers were significantly lower in the intermediate group. The percentage of secondary triggers was significantly larger in the older group than in the other two groups (0% in young vs 23% in intermediate vs 72% in older; $P < 0.0001$). Concerning the subdivision of secondary triggers on the basis of genotype, hypokalemia was only observed in LQT1, drugs mainly in LQT2, and AV block only in LQT2.**

Conclusion: **Arrhythmic triggers in LQTS differ depending on the age of the patients, stressing the importance of age-related therapy for genotyped LQTS patients.** *(J Cardiovasc Electrophysiol, Vol. 19, pp. 794-799, August 2008)*

long QT syndrome, genetic test, age, triggers, drugs, hypokalemia, bradycardia

Introduction

The long QT syndrome (LQTS) is a disease entity characterized by an abnormality in the myocardial repolarization that leads to the prolongation of the QT interval, morphological changes in T waves, and torsade de pointes (TdP) type of ventricular tachycardia on surface electrocardiogram (ECG).[1] The prevalence of LQTS is reported as 1 per 5,000 and it induces syncope and sudden cardiac death usually among young people. Up to date, several different genes have been reported to cause the LQTS.[1-3]

Since the first description on two LQTS-related genes (*KCNH2* and *SCN5A*) in 1995,[1] a number of studies have been performed regarding the relationship between genotype and phenotype. In addition to the genetic background predisposing excessive QT prolongation and TdP, many triggers have been known to modify and aggravate the clinical features of LQTS.[4,5] They are, for example, gender (being female), exercise, emotional stress, loud noise, sudden arousal, drugs, hypokalemia, and bradycardia. Some of them are related to the autonomic nervous tone, and it is well known that LQT1 patients are at a higher risk of TdP during exercise and LQT2 patients, in sudden arousal and auditory stimuli.[5-7]

Although many LQTS patients develop symptoms during adolescence, some of them experience the first cardiac event in their adulthood. In order to study the age-related difference in the LQTS phenotype, we aimed to examine whether the above-mentioned triggers for cardiac events are different depending on the age in genotyped and symptomatic LQTS patients.

This work was supported by research grants from the Ministry of Education, Science, Sports and Culture of Japan and Health Sciences Research Grants (H18 – Research on Human Genome – 002) from the Ministry of Health, Labour and Welfare, Japan, to Drs. Shimizu and Horie.

The first two authors contributed equally to the original concept and to the authorship of this investigation.

Address for correspondence: Minoru Horie, M.D., Ph.D., Department of Cardiovascular Medicine, Shiga University of Medical Science, Seta Tsukinowa, Otsu, Shiga, 520-2192, Japan. Fax: +81-77-543-5839; E-mail: horie@belle.shiga-med.ac.jp

Manuscript received 3 October 2007; Revised manuscript received 28 January 2008; Accepted for publication 4 February 2008.

doi: 10.1111/j.1540-8167.2008.01138.x

Methods

Study Population

The study population consisted of consecutive 145 symptomatic patients (117 probands and 28 family members) of a known genotype (LQT1, LQT2, and LQT3) from 117 unrelated Japanese families out of 343 genotyped patients (185 probands and 158 family members). They were enrolled from three institutes in Japan – Shiga University of Medical Science, National Cardiovascular Center, and Kyoto University Graduate School of Medicine – between 1996 and 2007. Patients with LQT5, LQT6, LQT7 (Andersen-Tawil syndrome), and compound mutations were excluded from the present study. All of the patients experienced cardiac events, and they were associated with, or triggered by, well-defined conditions. LQTS-related cardiac events were defined as syncope (transient and complete loss of consciousness), documented TdP, aborted cardiac arrest, or unexpected sudden cardiac death without a known cause. We excluded the patients who were genotyped but remained asymptomatic. All subjects or their guardians provided informed consent for the genetic and clinical studies according to each institutional review board's guidelines.

The patients were classified into three groups according to the age of first onset of cardiac events: (1) young group (n = 106): patients who experienced their first cardiac event at age of less than 20 years; (2) intermediate group (n = 20): those who experienced their first cardiac event at age of 20-39 years; and (3) older group (n = 19): those who experienced their first cardiac event after age of 40 years.

Clinical Phenotyping

Routine clinical and electrocardiographic (ECG) parameters were acquired at the time of the first examination for the evaluation of LQTS. Measured parameters on the first recorded ECG included QT and R-R interval in milliseconds, with corrected QT interval (QTc) corrected for heart rate (HR) by Bazett's formula.[8] Measurement for ECG parameters was performed manually on lead V5 (if not available on leads II). A cumulative LQTS diagnostic "Schwartz" score (which is derived in part from the QTc, symptoms, and family history) was assigned.[9] In regard to the family history, we defined positive family history as subjects who have relatives with a Schwartz score of ≥4.

Genetic Analysis

Screening for mutations of *KCNQ1*, *KCNH2*, and *SCN5A* was performed using polymerase chain reaction (PCR)/single-strand conformation polymorphism (SSCP) or denatured high-performance liquid chromatography analyses (dHPLC, WAVE system; Transgenomic Inc., Omaha, NE, USA). For aberrant PCR products, DNA sequencing was conducted with a DNA sequencer (ABI 3130 DNA Sequencer; Perkin Elmer, Foster City, CA, USA).

Genetic mutations of amino acid sequence were characterized by a specific location and coding effect (missense, nonsense, splice site, frameshift, insertion, deletion, and intronic variant). The transmembrane regions of *KCNQ1*, *KCNH2*, and *SCN5A* were defined as six membrane segments (S1 to S6, amino acid residues 112 through 354 for *KCNQ1*, 397 through 666 for *KCNH2*, and 127 through 1771 for *SCN5A*, respectively). They, therefore, included cytoplasmic and extracellular linkers, as well as the pore region. As for LQT1 and LQT2, the pore region was defined as the area extending from S5 to the mid portion of S6 involving amino acid residues 262 through 354 for *KCNQ1* and 550 through 650 for *KCNH2*, respectively.[10-14]

Triggering Factors

We divided the triggers into three categories:(1) adrenergically mediated triggers: exercise, emotional stress, loud noise, and arousal; (2) vagally mediated triggers: rest/sleep; and (3) secondary triggers: drugs, hypokalemia, and AV block. There was a small number of undefined conditions associated with cardiac events, and they were classified as other triggers and excluded for analysis in Figures 1–3.

Statistical Analysis

Data are expressed as the mean value ± standard deviation (SD). The clinical characteristics of the study groups were compared with the chi-square test for categorical variables. For continuous variables, we analyzed the normally distributed data with one-way analysis of variance and non-normally distributed data with Kruskal-Wallis tests. For comparisons between two groups, the Student's *t*-test was used for parametric data and the Mann–Whitney's *U*-test for non-parametric data. Differences were accepted as significant for P value of <0.05.

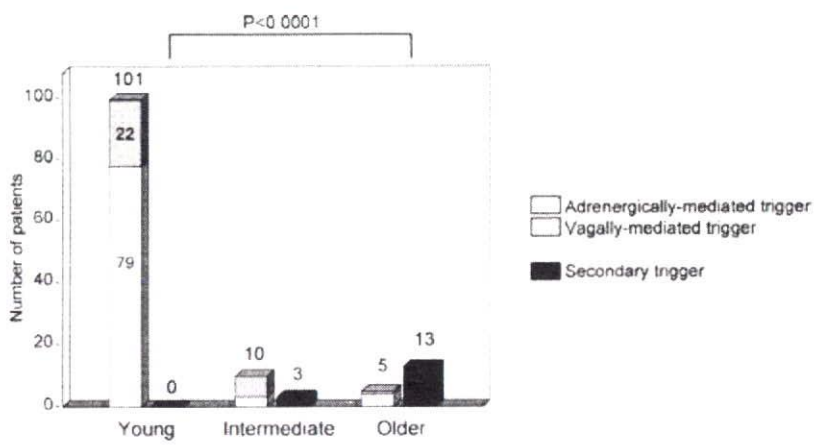

Figure 1. *Triggers for cardiac events in the young, intermediate, and older groups. Incidence of three categorical triggers. Bar graphs show the number of symptomatic patients and their triggers of the first cardiac events: open bars, adrenergically mediated; gray bars, vagally mediated; and black bars, secondary triggers. Other triggers for cardiac events that were undefined were excluded.*

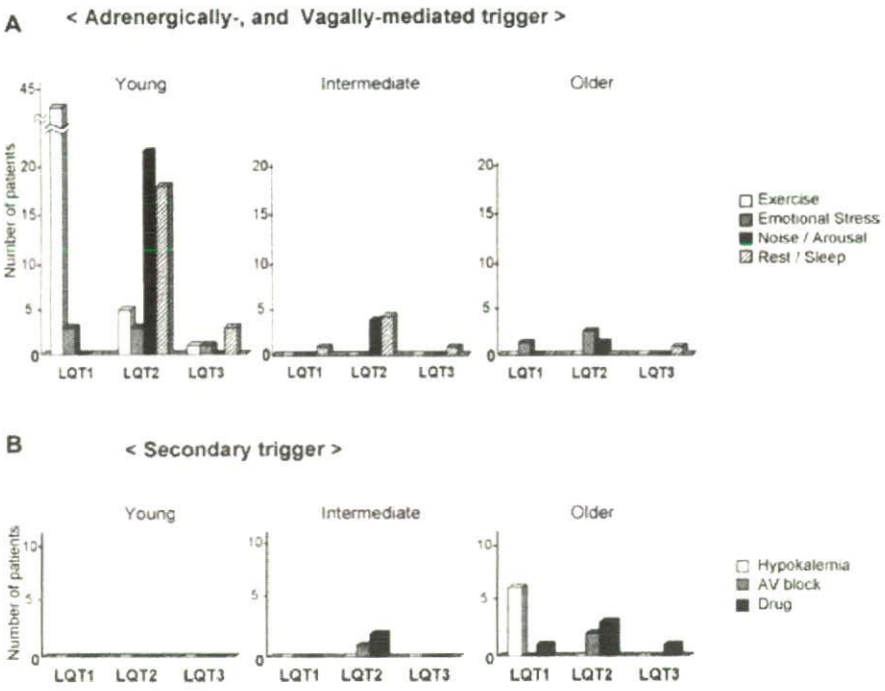

Figure 2. *Genotype-dependent difference of triggers for cardiac events in the young, intermediate, and older groups. A: autonomic triggers, B: secondary triggers; bar graphs indicate the number of patients and their patterns of a specific trigger as summarized in insets. Other triggers for cardiac events that were undefined were excluded.*

Results

Clinical Characteristics

Table 1 summarizes the clinical characteristics of the study subjects. The percentages of females, probands, and patients with positive family history were significantly different among the three groups. In the older group, the percentage of females and probands increased, but that of positive family history decreased. The intermediate group patients showed similar levels of QT prolongation, family history, and Schwartz scores as those of the young group patients. There were no significant differences in basal HR, QTc, and Schwartz scores among the three groups.

Genetic Characteristics

There were 58 LQT1, 75 LQT2, and 12 LQT3 patients (Table 1). In these genotyped patients, we identified 31 *KCNQ1*, 60 *KCNH2*, and 8 *SCN5A* mutations (total 99 different mutations). Among 58 LQT1 patients, most (48/58, 83%) of the first cardiac events occurred at young age. In contrast, first cardiac events occurred less at young age in LQT2 (51/75, 68%) and LQT3 (7/12, 58%) patients compared to the LQT1 patients ($P = 0.019$). The prevalence of transmembrane mutations in LQT1 and LQT3 patients and that of pore site mutations in LQT2 patients was evaluated, but no significant differences were observed among the three groups.

Triggers for Cardiac Events

Figure 1 illustrates the incidence of three categorical triggers in the three age groups. In Figure 1, left-sided bars indicate the number of patients in whom the event was induced by either adrenergically (open bar) or vagally (gray bar) mediated triggers. Right-sided black bars indicate those with secondary triggers. The vertical axis indicates the number of patients. In the young group, all 101 cardiac events were

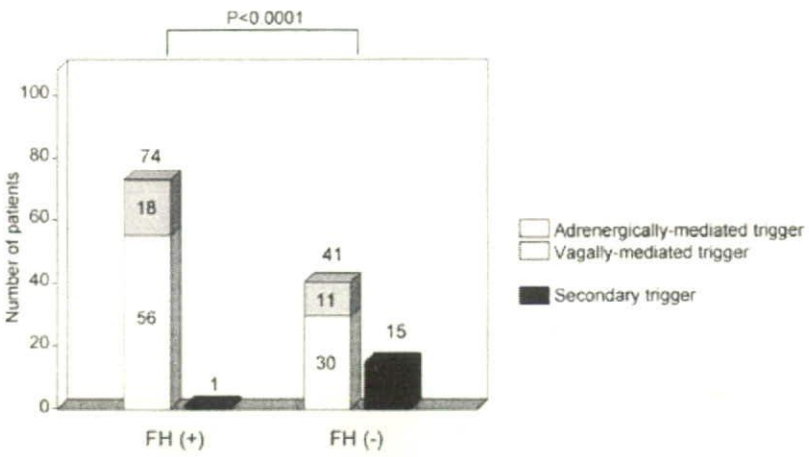

Figure 3. *Triggers for cardiac events in the patients with and without family history. Bar graphs show the number of symptomatic patients and their triggers to induce the cardiac events: open bars, adrenergically mediated; gray bars, vagally mediated; and black bars, secondary triggers. Other triggers for cardiac events that were undefined were excluded.*

TABLE 1

Clinical and Genetic Characteristics in the Three Groups

	Young (n = 106)	Intermediate (n = 20)	Older (n = 19)	P Value
Age at first cardiac event (years)	11.0 ± 0.4	28.0 ± 1.1	59.0 ± 3.5	
Female (%)	63 (59%)	16 (80%)	18 (95%)	0.004
Proband (%)	80 (75%)	18 (90%)	19 (100%)	0.035
Family history	68 (64%)	11 (55%)	3 (16%)	<0.001
HR (bpm)	65 ± 1.2	65 ± 2.8	65 ± 2.8	0.984
QTc (ms)	515 ± 5.7	523 ± 12	485 ± 10	0.084
Schwartz score	6.1 ± 0.2	6.2 ± 0.4	5.3 ± 0.5	0.335
Subtype				
LQT1 (n = 58)	48/58 (83%)	1/58 (2%)	9/58 (15%)	
LQT2 (n = 75)	51/75 (66%)	16/75 (21%)	8/75 (11%)	
LQT3 (n = 12)	7/12 (58%)	3/12 (25%)	2/12 (17%)	
Transmembrane mutation (LQT1)	39/48 (81%)	1/1 (100%)	7/9 (78%)	
Pore site mutation (LQT2)	25/51 (49%)	9/16 (56%)	1/8 (13%)	
Transmembrane mutation (LQT3)	6/7 (86%)	3/3 (100%)	1/2 (50%)	

Data are presented as the mean value ± SD or number (%) of subjects.
HR = heart rate; LQT1 = long QT syndrome caused by the *KCNQ1* potassium channel gene mutations; LQT2 = long QT syndrome caused by the *KCNH2* potassium channel gene mutations; LQT3 = long QT syndrome caused by the *SCN5A* sodium channel gene mutations; QTc = QT interval corrected by Bazett's formula.

TABLE 2

Clinical and Genetic Characteristics in Patients With or Without Family History

	FH (+) (n = 82)	FH (−) (n = 63)	P Value
Age at first cardiac event (years)	14.0 ± 1.1	26.0 ± 2.8	<0.001
Female (%)	55 (67%)	42 (67%)	0.960
Proband (%)	54 (66%)	63 (100%)	<0.001
HR (bpm)	65 ± 1.2	64 ± 1.4	0.728
QTc (ms)	512 ± 6.9	513 ± 7.0	0.890
Schwartz score	6.4 ± 0.2	5.6 ± 0.2	0.005
Subtype			
LQT1 (n = 58)	40/58 (69%)	18/58 (31%)	
LQT2 (n = 75)	36/75 (48%)	39/75 (52%)	
LQT3 (n = 12)	6/12 (50%)	6/12 (50%)	
Transmembrane mutation (LQT1)	35/40 (88%)	13/18 (72%)	
Pore site mutation (LQT2)	19/36 (53%)	16/39 (41%)	
Transmembrane mutation (LQT3)	6/6 (100%)	4/6 (67%)	

Data are presented as the mean value ± SD or number (%) of subjects.
FH = family history; HR = heart rate; LQT1 = long QT syndrome caused by the *KCNQ1* potassium channel gene mutations; LQT2 = long QT syndrome caused by the *KCNH2* potassium channel gene mutations; LQT3 = long QT syndrome caused by the *SCN5A* sodium channel gene mutations; QTc = QT interval corrected by Bazett's formula.

associated with autonomic triggers, among which 79 (78%) events were adrenergically mediated and 22 (22%) were vagally mediated. On the other hand, only 5 of 18 cardiac events (28%) were associated with autonomic triggers in the older group, and secondary triggers induced cardiac events in the majority of the older group patients (13/18, 72%). The percentage of secondary triggers was significantly larger in the older group than in the other two groups (0% in young [0/101] vs 23% in intermediate [3/13] vs 72% in older [13/18]; $P < 0.0001$). Among the cardiac events triggered by autonomic factors, the percentage of the adrenergically mediated triggers was significantly lower in the intermediate group patients (79/101 [78%] in young vs 3/10 [30%] in intermediate vs 4/5 [80%] in older group; $P < 0.001$). Thus, triggering factors were significantly different among the three groups.

Figure 2A shows autonomic triggers in the three genotypes in each age group. There were also genotype-dependent differences in triggers for cardiac events in the young group, as previously reported:[5] in young LQT1 patients, 92% (44/48) of the cardiac events occurred during exercise (open bar), but none with noise/arousal (black bar) or rest/sleep (hatched bar). This is in sharp contrast with the pattern in young LQT2 patients: 37% (19/51) of the events occurred during rest/sleep and 43% (22/51) with noise/arousal. Irrespective of onset age, cardiac events triggered by noise/arousal were very specific and observed in only LQT2 patients (35%, 26 of 75 LQT2 patients). In contrast, 44% (3/7) of LQT3 patients experienced cardiac events during rest/sleep. In opposition to the young LQT1 patients, only ~20% of total LQT2 and LQT3 patients experienced cardiac events triggered by exercise or emotional stress.

Figure 2B depicts secondary triggers in the three genotypes in each age group. Hypokalemia (open bar), complete AV block (gray), and drugs (black) were associated with cardiac events in total of 6, 3, and 7 patients, respectively, in the intermediate and older groups. Interestingly, hypokalemia was associated with cardiac episodes in only older LQT1 patients. On the other hand, drugs and AV block triggered cardiac events mainly in LQT2 patients of >20 years. Responsible drugs were amphetamine, aprindine, cisapride (plus pirmenol), disopyramide, erythromycin, hydroxyzine, and procainamide.

Family History

Comparison of clinical and genetic characteristics between patients with and without family history is shown in Table 2. The age at first cardiac event was significantly younger and Schwartz score was significantly higher in the patients with family history than in those without it. LQT1 patients appeared to have more family history compared to those of LQT2 and LQT3 genotypes. Figure 3 illustrates the incidence of three categorical triggers in patients with and without family history. Triggers for cardiac events were also significantly different between the two groups, and secondary trigger was seen in only 1 patient with family history and in 27% (15 of 56) of patients without family history.

Discussion

In the genotyped/symptomatic LQTS patients, the present study demonstrated that factors triggering cardiac events were different depending on the age of their first onset. In general, syncope and sudden death in LQTS are believed to be due to TdP-type of ventricular tachycardia and occur usually in the young.[15,16] However, pathophysiological properties of LQTS-related events were found to be even different among the three groups that were divided by age of less than 20, 20-39, and greater than 40 years. In the young group (<20 years), triggers were closely related to the autonomic nervous tone. In contrast, secondary triggers induced cardiac events in 72% of the older patients (>40 years), suggesting

that "double hit" by secondary trigger(s) appeared to aggravate the clinical phenotype, in addition to genetic variants in ion channel genes, in the older group. The intermediate group patients were at in-between risk in clinical characteristics and the triggers of cardiac events. Interestingly, regarding the triggers of cardiac events, the percentage of the adrenergically mediated trigger was lower in the intermediate group. This may reflect a relatively small number of LQT1 patients in the intermediate group.

Although there was no statistically significant difference in the QTc interval among the three age groups ($P = 0.084$), the older group showed shorter QTc interval compared to that in the other two groups. The QTc in the young group was even shorter than that in the intermediate group. This was probably due to the fact that the QTc in the LQT1 patients was significantly shorter than that in the LQT2 and LQT3 patients (LQT1: 490 ± 6.6, LQT2: 534 ± 8.4, LQT3: 555 ± 26; $P < 0.0001$) and the percentage of LQT1 patients was higher in the young group.

Our results in the young group are consistent with previous reports:[5,7] LQT1 patients experienced the majority of their cardiac events during exercise or emotional stress and only a few occurred during rest/sleep, in opposition to the pattern in LQT2 and LQT3 patients. Cardiac events in LQT2 patients in the young group were mainly associated with noise and sudden arousal and other adrenergic triggers. Cardiac events occurred during rest/sleep in half of the young LQT3 patients.

Among the secondary triggers, hypokalemia was associated with cardiac episodes in only LQT1 patients. Lower extracellular K^+ concentrations are known to reduce outward conductance of both rapid component of delayed rectifier potassium (I_{Kr}) and background inward rectifier potassium (I_{K1}) currents.[17-19] In LQT1, the slow component of delayed rectifier potassium current (I_{Ks}) is impaired, and the function of I_{Kr} and I_{K1} channels remains normal or even upregulated to compensate the total net outward K^+ conductance. Therefore, hypokalemia may unveil the potential repolarization disorder by reducing both "healthy" I_{Kr} and I_{K1}.

On the other hand, AV block and drug intake associated with cardiac events as secondary triggers were seen to be present in most of the intermediate and older LQT2 patients. Tan and colleagues[20] reported that pause-dependence of TdP onset was predominant in LQT2 but absent or rare in LQT1, suggesting that this disparity may reflect different mechanisms. Experimental studies have shown that I_{Ks} blockade (LQT1) causes delayed afterdepolarizations (DAD) but not early afterdepolarizations (EAD);[21] on the contrary, I_{Kr} blockade (LQT2) causes EADs, predominantly at slower HRs.[22] Extreme bradycardia due to AV block may lead to EAD as well as TdP through the postpausal prolongation of action potential plateau. Both a smaller I_{Kr} due to complete deactivation and an enhanced inward Na^+/Ca^{2+} exchanger at low HR may contribute to EAD formation by providing time for recovery and reactivation of L-type Ca^+ channel. In the presence of pathological bradycardia, therefore, I_{Kr} plays a more important role in abbreviating the repolarization and, thereby, keeping the appropriate QT interval because little accumulation of outward I_{Ks} occurs at lower HR.[23]

In this connection, drug-induced TdP has been shown to depend on intervals of preceding pauses.[24] The above-mentioned mechanism on the bradycardia-induced TdP may give an explanation of our result that most of the drug-induced events were observed in LQT2. Because responsible drugs are known to block cardiac I_{Kr} (except hydroxyzine), preexisting repolarization abnormality due to gene mutations may predispose the patients to fatal arrhythmias by further reducing the outward K^+ conductance.[25,26] In preliminary experiments of biophysical assay with heterologous expression systems, we found that these *KCNH2* mutations identified in drug-induced TdP patients produced mild loss-of-function of I_{Kr}.

We evaluated only "already-symptomatic" genotyped patients in this study. The percentage of "still-asymptomatic" patients was 58% of all genotyped patients (198 of 343). The average ages of asymptomatic patients were 19.0 ± 1.9 years (5–67 years) for probands and 34.0 ± 1.8 years (2–68 years) for family members. Asymptomatic probands were still young; therefore, some of them would be symptomatic in the future, being exposed to higher risk of lethal events. The results of our study again emphasize the importance of a careful approach to asymptomatic (preclinical) LQTS patients to decrease their arrhythmic risk, particularly in older patients (≥20 years). Because of lack of apparent phenotypes, most of them were not diagnosed prior to the onset of symptoms. However, one of the most important missions of our genetic testing would be to achieve a preclinical diagnosis of LQTS, particularly in patients with forme-fruste phenotype. Because of low penetrance, inheriting a gene mutation per se does not always mean that the individual mutation carrier will present clinical manifestation,[27] but apparently "healthy" carriers have inherited the risk for developing the clinical phenotype. Once genetic information becomes available, we can introduce the timely beta-blocker therapy and conduct careful follow-up, including ECG recordings, lifestyle modifications (i.e., avoidance of QT-prolonging drugs), avoidance of hyopokalemia, bradycardia, other alarming symptoms, and family education (home automatic electrical defibrillator, etc.).

Study Limitations

Intermediate and older group patients may have a higher possibility to use more drugs. We, therefore, could not exclude such an age-dependent risk accumulation affecting the results of trigger distribution. As for another issue, carriers of milder mutations may induce cardiac events more likely in association with secondary triggers. Our study included only subjects with three major genotypes, although they account for the majority of LQTS patients. Patients with compound mutations of LQT1-3 and 5–7 genotypes were all excluded from analysis. However, we failed to exclude compound mutation carriers with other (LQT4, 8–10) or unknown genotypes, which may result in a minor selection bias.

We evaluated only the Japanese population and there remains a concern about ethnic differences. However, the prevalent mutations found in more than 4 patients were A341V-KCNQ1, A344A/sp-KCNQ1, and A614V-HERG and were all popular in other ethnic cohorts. The genotype-specific triggers were also similar to those observed in previous studies from other countries.

Although syncope may result from diseases other than LQTS-related ventricular arrhythmia, we considered sudden onset/offset nature of loss of consciousness in a genotyped LQTS patient as syncope due to ventricular arrhythmias, if there was no evidence of another explanation, and included as a study subject. In this connection, very short duration of

TdP that did not cause syncope was underestimated if Holter ECG failed to detect it.

Conclusion

Triggers of cardiac events were closely related to the autonomic nervous tone with a higher incidence of family history in younger patients. In contrast, arrhythmic events in older patients were associated with secondary triggers, such as drugs, hypokalemia, and AV block, with genotype specificity. Thus, arrhythmic triggers in LQTS differ depending on the age of the patients, stressing the importance of age- and genotype-related therapy for genotyped LQTS.

Acknowledgments: We gratefully acknowledge the technical assistance of Arisa Ikeda, Tamami Hirata (Department of Cardiovascular Medicine, Shiga University of Medical Science, Otsu, Japan), Toshiko Shibata, Naotaka Ohta, and Toshiro Ura (Laboratory of Molecular Genetics, National Cardiovascular Center, Suita, Japan).

References

1. Shimizu W: The long QT syndrome: Therapeutic implications of a genetic diagnosis. Cardiovasc Res 2005;67:347-356.
2. Vatta M, Ackerman MJ, Ye B, Makielski JC, Ughanze EE, Taylor EW, Tester DJ, Balijepalli RC, Foell JD, Li Z, Kamp TJ, Towbin JA: Mutant caveolin-3 induces persistent late sodium current and is associated with long-QT syndrome. Circulation 2006;114:2104-2112.
3. Medeiros-Domingo A, Kaku T, Tester DJ, Iturralde-Torres P, Itty A, Ye B, Valdivia C, Ueda K, Canizales-Quinteros S, Tusié-Luna MT, Makielski JC, Ackerman MJ: SCN4B-encoded sodium channel beta4 subunit in congenital long-QT syndrome. Circulation 2007;116:134-142.
4. Schwartz PJ, Priori SG, Locati EH, Napolitano C, Cantù F, Towbin JA, Keating MT, Hammoude H, Brown AM, Chen LS: Long QT syndrome patients with mutations of the *SCN5A* and *HERG* genes have differential responses to Na^+ channel blockade and to increases in heart rate. Implications for gene-specific therapy. Circulation 1995;92:3381-3386.
5. Schwartz PJ, Priori SG, Spazzolini C, Moss AJ, Vincent GM, Napolitano C, Denjoy I, Guicheney P, Breithardt G, Keating MT, Towbin JA, Beggs AH, Brink P, Wilde AA, Toivonen L, Zareba W, Robinson JL, Timothy KW, Corfield V, Wattanasirichaigoon D, Corbett C, Haverkamp W, Schulze-Bahr E, Lehmann MH, Schwartz K, Coumel P, Bloise R: Genotype-phenotype correlation in the long-QT syndrome: Gene-specific triggers for life-threatening arrhythmias. Circulation 2001;103:89-95.
6. Schwartz PJ, Zara A, Locati E, Moss AJ: Stress and sudden death. The case of long QT syndrome. Circulation 1991;83(Suppl II):II70-II80.
7. Wilde AA, Jongbloed RJ, Doevendans PA, Düren DR, Hauer RN, van Langen IM, van Tintelen JP, Smeets HJ, Meyer H, Geelen JL: Auditory stimuli as a trigger for arrhythmic events differentiate *HERG*-related (LQTS2) patients from *KVLQT1*-related patients (LQTS1). J Am Coll Cardiol 1999;33:327-332.
8. Bazett HC: An analysis of the time-relations of electrocardiograms. Heart 1920;7:353-370.
9. Schwartz PJ, Moss AJ, Vincent GM, Crampton RS: Diagnostic criteria for the long QT syndrome: An update. Circulation 1993;88:782-784.
10. Shimizu W, Horie M, Ohno S, Takenaka K, Yamaguchi M, Shimizu M, Washizuka T, Aizawa Y, Nakamura K, Ohe T, Aiba T, Miyamoto Y, Yoshimasa Y, Towbin JA, Priori SG, Kamakura S: Mutation site-specific differences in arrhythmic risk and sensitivity to sympathetic stimulation in the LQT1 form of congenital long QT syndrome: Multicenter study in Japan. J Am Coll Cardiol 2004;44:117-125.
11. Moss AJ, Shimizu W, Wilde AA, Towbin JA, Zareba W, Robinson JL, Qi M, Vincent GM, Ackerman MJ, Kaufman ES, Hofman N, Seth R, Kamakura S, Miyamoto Y, Goldenberg I, Andrews ML, McNitt S: Clinical aspects of type-1 long-QT syndrome by location, coding type, and biophysical function of mutations involving the *KCNQ1* gene. Circulation 2007;115:2481-2489.
12. Moss AJ, Zareba W, Kaufman ES, Gartman E, Peterson DR, Benhorin J, Towbin JA, Keating MT, Priori SG, Schwartz PJ, Vincent GM, Robinson JL, Andrews ML, Feng C, Hall WJ, Medina A, Zhang L, Wang Z: Increased risk of arrhythmic events in long-QT syndrome with mutations in the pore region of the human ether-a-go-go-related gene potassium channel. Circulation 2002;105:794-799.
13. Splawski I, Shen J, Timothy KW, Vincent GM, Lehmann MH, Keating MT: Genomic structure of three long QT syndrome genes: *KVLQT1*, *HERG*, and *KCNE1*. Genomics 1998;51:86-97.
14. Wang Q, Li Z, Shen J, Keating MT: Genomic organization of the human *SCN5A* gene encoding the cardiac sodium channel. Genomics 1996;34:9-16.
15. Zareba W, Moss AJ, Schwartz PJ, Vincent GM, Robinson JL, Priori SG, Benhorin J, Locati EH, Towbin JA, Keating MT, Lehmann MH, Hall WJ: Influence of the genotype on the clinical course of the long-QT syndrome. N Engl J Med 1998;339:960-965.
16. Priori SG, Schwartz PJ, Napolitano C, Bloise R, Ronchetti E, Grillo M, Vicentini A, Spazzolini C, Nastoli J, Bottelli G, Folli R, Cappelletti D: Risk stratification in the long-QT syndrome. N Engl J Med 2003;348:1866-1874.
17. Lopez-Barneo J, Hoshi T, Heinemann SH, Aldrich RW: Effects of external cations and mutations in the pore region on C-type inactivation of Shaker potassium channels. Receptors Channels 1993;1:61-71.
18. Choy AM, Lang CC, Chomsky DM, Rayos GH, Wilson JR, Roden DM: Normalization of acquired QT prolongation in humans by intravenous potassium. Circulation 1997;96:2149-2154.
19. Rasmusson RL, Morales MJ, Wang S, Liu S, Campbell DL, Brahmajothi MV, Strauss HC: Inactivation of voltage-gated cardiac K^+ channels. Circ Res 1998;82:739-750.
20. Tan HL, Bardai A, Shimizu W, Moss AJ, Schulze-Bahr E, Noda T, Wilde AAM: Genotype-specific onset of arrhythmias in congenital long-QT syndrome: Possible therapy implications. Circulation 2006;114:2096-2103.
21. Burashnikov A, Antzelevitch C: Block of $I_{(Ks)}$ does not induce early afterdepolarization activity but promotes beta-adrenergic agonist-induced delayed afterdepolarization activity. J Cardiovasc Electrophysiol 2000;11:458-465.
22. Liu J, Laurita KR: The mechanism of pause-induced torsade de pointes in long QT syndrome. J Cardiovasc Electrophysiol 2005;16:981-987.
23. Stengl M, Volders PGA, Thomsen M, Spatjens RL, Sipido KR, Vos MA: Accumulation of slowly activating delayed rectifier potassium current (I_{Ks}) in canine ventricular myocytes. J Physiol 2003;551:777-786.
24. Tan HL, Hou CJ, Lauer MR, Sung RJ: Electrophysiologic mechanisms of the long QT interval syndromes and torsade de pointes. Ann Intern Med 1995;122:701.
25. Sanguinetti MC, Jiang C, Curran ME, Keating MT: A mechanistic link between an inherited and an acquired cardiac arrhythmia: *HERG* encodes the I_{Kr} potassium channel. Cell 1995;81:299-307.
26. Mitcheson JS, Chen J, Lin M, Culberson C, Sanguinetti MC: A structural basis for drug-induced long QT syndrome. Proc Natl Acad Sci U S A 2000;97:12329-12333.
27. Priori SG, Napolitano C, Schwartz PJ: Low penetrance in the long-QT syndrome clinical impact. Circulation 1999;99:529-533.

α-1-Syntrophin Mutation and the Long-QT Syndrome
A Disease of Sodium Channel Disruption

Geru Wu, MD, PhD; Tomohiko Ai, MD, PhD; Jeffrey J. Kim, MD; Bhagyalaxmi Mohapatra, PhD; Yutao Xi, PhD; Zhaohui Li, MD, PhD; Shahrzad Abbasi, MS; Enkhsaikhan Purevjav, MD, PhD; Kaveh Samani, MD; Michael J Ackerman, MD, PhD; Ming Qi, PhD; Arthur J. Moss, MD; Wataru Shimizu, MD; Jeffrey A. Towbin, MD; Jie Cheng, MD, PhD; Matteo Vatta, PhD

Background—Long-QT syndrome (LQTS) is an inherited disorder associated with sudden cardiac death. The cytoskeletal protein syntrophin-α_1 (SNTA1) is known to interact with the cardiac sodium channel ($hNa_v1.5$), and we hypothesized that SNTA1 mutations might cause phenotypic LQTS in patients with genotypically normal $hNa_v1.5$ by secondarily disturbing sodium channel function.

Methods and Results—Mutational analysis of *SNTA1* was performed on 39 LQTS patients (QTc≥480 ms) with previously negative genetic screening for the known LQTS-causing genes. We identified a novel A257G-*SNTA1* missense mutation, which affects a highly conserved residue, in 3 unrelated LQTS probands but not in 400 ethnic-matched control alleles. Only 1 of these probands had a preexisting family history of LQTS and sudden death with an additional intronic variant in KCNQ1. Electrophysiological analysis was performed using HEK-293 cells stably expressing $hNa_v1.5$ and transiently transfected with either wild-type or mutant SNTA1 and, in neonatal rat cardiomyocytes, transiently transfected with either wild-type or mutant SNTA1. In both HEK-293 cells and neonatal rat cardiomyocytes, increased peak sodium currents were noted along with a 10-mV negative shift of the onset and peak of currents of the current-voltage relationships. In addition, A257G-SNTA1 shifted the steady-state activation (V_h) leftward by 9.4 mV, whereas the voltage-dependent inactivation kinetics and the late sodium currents were similar to wild-type SNTA1.

Conclusion—*SNTA1* is a new susceptibility gene for LQTS. A257G-*SNTA1* can cause gain-of-function of $Na_v1.5$ similar to the LQT3. (***Circ Arrhythmia Electrophysiol.* 2008;1:193-201.**)

Key Words: arrhythmia ■ death, sudden (if surviving, use heart arrest) ■ ion channels ■ long-QT syndrome

Long-QT syndrome (LQTS) is an inherited disorder that can cause sudden cardiac death. To date, hundreds of genetic mutations and single nucleotide polymorphisms in 11 distinct LQTS-susceptibility genes have been reported. Electrophysiological studies using in vitro cell expression systems and genetically engineered animal models have suggested that "gain of function" or "loss of function" in the ion channels that are essential to generate action potentials may account for the LQTS phenotypes.[1] The functional modifications of the ion channels are primarily caused by defects in the genes encoding the pore-forming subunits (*KCNQ1*, *KCNH2*, *SCN5A*, *KCNJ2*, and *CACNA1C*) or the β subunits (*KCNE1*, *KCNE2*, and *SCN4B*) of the ion channels except for the gene responsible for LQT4.[2] Unlike the other genes, LQT4 is caused by the malfunction of ankyrin B that is involved in the cellular organization of the sodium/calcium exchanger and inositol-1,4.5-triphosphate receptors.[3]

Clinical Perspective see p 201

However, in 20% to 30% of cases, genetic analysis fails to identify the responsible gene for the LQTS phenotypes in affected patients.[4] Recently, Vatta et al and Cronk et al reported that mutations in caveolin-3 identified in the patients with LQTS or the infants succumbing to sudden infant death syndrome can affect human cardiac sodium channel ($hNa_v1.5$) gating kinetics and generate sustained currents, probably by direct protein–protein interactions.[5,6] In addition, mutations in the A-kinase anchoring protein 9 gene (*AKAP9*) have been identified in LQTS.[7] AKAP9 determines the subcellular localization of protein kinase A and the phosphor-

Received January 28, 2008; accepted May 12, 2008.

From the Electrophysiology Research Laboratory, Texas Heart Institute/St. Luke's Episcopal Hospital, Houston, Tex (G.W., T.A., Y.X., S.A., K.S., J.C.); Pediatric Cardiology, Texas Children's Hospital/Baylor College of Medicine, Houston, Tex (J.J.K., B.M., Z.L., E.P., J.A.T., M.V.); Departments of Medicine, Pediatrics, and Molecular Pharmacology and Experimental Therapeutics/Divisions of Cardiovascular Diseases and Pediatric Cardiology, Mayo Clinic, Rochester, Minn (M.J.A.); Heart Research Follow-up Program, University of Rochester Medical Center, Rochester, NY (M.Q., A.J.M.); Division of Cardiology, National Cardiovascular Center, Suita, Japan (W.S.).

The online-only Data Supplement is available with this article at http://circ.ahajournals.org/cgi/content/full/CIRCEP.108.769224/DCI.

Presented in part at the 2007 American Heart Association (AHA) Annual Scientific Sessions, Orlando, Fla.

Correspondence to Matteo Vatta, PhD, BCM/TCH, 1102 Bates St, F.C. 430.04, Houston, TX 77030. E-mail mvatta@bcm.tmc.edu or Tomohiko Ai, MD, PhD, THI/SLEH, 6770 Bertner Ave, MC 2–255, Houston, TX 77030. E-mail tomohikoai@yahoo.com

Circ Arrhythmia Electrophysiol **is available at http://circep.ahajournals.org** **DOI: 10.1161/CIRCEP.108.769224**

ylation of the I_{Ks} potassium channel α subunit (KCNQ1) to which it assembles.[8] These studies proposed a novel concept that the defects of non–ion channel proteins or channel-interacting proteins can affect ion-channel gating kinetics, thereby causing secondary channel dysfunction leading to LQTS. Hence, this concept uncovers a cascade or domino effect that disturbs the "final common pathway"[9] that causes arrhythmias, ion channels, and focuses attention on a novel class of proteins and candidate genes to explain the residual 25% of LQTS that remain genotype negative.

Syntrophins are cytoplasmic submembranous proteins that are components of the dystrophin-associated protein complex.[7] Several syntrophin isoforms (α_1, β_1, β_2, γ_1, and γ_2) have been identified in the heart, skeletal muscle, and neurons.[10–14] The PDZ domain of syntrophin-α_1 (SNTA1), the most abundant isoform in the heart, has been reported to bind to the C-terminal domain of murine cardiac voltage-gated sodium channels (*SkM2*).[15] Ou et al demonstrated that syntrophin-γ_2 (SNTG2) affects hNa$_v$1.5 gating kinetics by protein–protein interaction via PDZ [postsynaptic density protein (PSD95), drosophila disc large tumor suppressor (DlgA), and zonula occludens-1 protein (zo-1)] domain in the distal C-terminus of the *SCN5A*-encoded sodium channel pore-forming subunit.[16] Notably, SNTG2 shares structural similarity with SNTA1. These observations led us to hypothesize that *SNTA1* might be a new candidate gene responsible for the LQTS in patients whose genetic screenings were negative for the already known subtypes operating by secondary disruption of sodium channel function.

Methods

Patients Demographics and Genetic Screening

We previously enrolled 364 unrelated probands clinically diagnosed with LQTS.[5] Among them, 39 genotype-negative LQTS patients (26 females; 66.7%) presenting with a resting QTc≥480 ms and a LQTS diagnostic score ≥3 were selected for further investigation.[17] All patients underwent physical examination, family history, and ECG analysis. The average age at diagnosis was 23.6 ± 6.3 years (range, 1–84 years), and the average QTc was 537 ± 19 ms (range, 480–670 ms).

Blood was obtained after written informed consent was obtained from all subjects. Genomic DNA was extracted from peripheral blood lymphocytes as previously described.[5] Using polymerase chain reaction and direct DNA sequencing, open reading frame/splice site mutational analysis was performed on the *SNTA1* gene (chromosome 20q11.2; 8 exons). Polymerase chain reaction amplification was performed using primers designed to flank the regions of this gene. All patients were, also, screened for the known LQTS-susceptibility genes (LQT1–9). All *SNTA1* genetic variants regarded as putative LQTS-associated mutations were required to change a conserved residue or splice site, altering the primary amino acid structure of the encoded protein. In addition, these genetic variants were required to be absent in at least 400 ethnic-matched reference alleles to be considered as mutations. Synonymous single nucleotide polymorphisms were excluded from consideration.

SNTA1 Gene Synthesis and Mutagenesis

Wild-type (WT) human *SNTA1* was synthesized based on the previously deposited sequence (GenBank Accession No. NM_003098; GenScript Corporation, Piscataway, NJ) and subcloned into the pcDNA3.1/CT-GFP-TOPO vector (Invitrogen, Carlsbad, CA). Site-directed mutagenesis was performed with the QuikChange Site-Directed Mutagenesis Kit (Stratagene, La Jolla, CA) by using the vector containing the WT-*SNTA1* as a template. The primers used for the mutagenesis are available on request. Polymerase chain reaction and bacteria transformations were performed according to the manufacturer's instructions. The mutated A257G-*SNTA1* clones were sequenced to ensure the presence of the mutation and the absence of other substitutions introduced by DNA polymerase.

HEK-293 Cell Preparation and Transient Expression of WT and Mutant SNTA1

Stable HEK-293 cell lines expressing consistent sodium currents were established from a single cell transfected with the vector containing Flag-tagged hNa$_v$1.5 (clone cells). The clone cells were transiently transfected with the vector containing WT- or A257G-SNTA1 using the Lipofectamine 2000 transfection reagent (Qiagen, Valencia, CA). To express β_1-subunit of human cardiac sodium channel (hβ_1), the clone cells were transiently transfected with the pIRES vector carrying hβ_1 and CD8 (kindly provided by Dr. Naomasa Makita, Hokkaido University, Sapporo, Japan) in conjunction with SNTA1. The cells were incubated at 37°C for 2 to 3 days before use.

Neonatal Rat Cardiomyocyte Isolation and Transient Expression of WT and Mutant SNTA1

All procedures were approved by the Institutional Animal Care and Use Committee at the Texas Heart Institute. Neonatal rat cardiomyocytes were isolated according to the procedures described elsewhere (see Methods in the supplemental material).

Patch-Clamp Experiments

Patch-clamp experiments were performed as previously described.[18] Macroscopic sodium currents were recorded at ambient temperature (22 to 24°C). Step-pulse voltages were generated with Axopatch 200B amplifier using pClamp9.0 software (Axon Instruments, Sunnyvale, CA). Currents were filtered at 10 kHz with a built-in 4-pole Bessel filter and fed to a computer at a sampling frequency of 20 kHz. (The details are described in the supplemental material.)

Coimmunoprecipitation

Coimmunoprecipitation was performed in HEK-293 cells stably expressing Flag-tagged hNa$_v$1.5 and transfected with either green fluorescent protein (GFP)-tagged WT-SNTA1 or A257G-SNTA1 as previously reported (see Methods in the supplemental material).[8]

Immunohistochemistry

Immunohistochemical staining was performed by standard techniques described elsewhere. Briefly, the HEK-293 cells stably expressing hNa$_v$1.5 were transfected with GFP-tagged WT-SNTA1. The cells were fixed with 4% paraformaldehyde, incubated with 0.5% Triton X-100, then sequentially stained with anti-SCN5A sodium channel antibody (1:100 dilution, Santa Cruz sc-23174) for 1 hour at room temperature, biotinylated antigoat IgG (1:100 dilution, VECTOR BA-2000) for 30 minutes, and antistreptavidin conjugated with Texas Red (1:100 dilution, ZYMED 43 to 4317) for 30 minutes. The results were examined with TCS-SP2 confocal laser-scanning microscope (Leica Microsystems).

Data Analysis

The sodium channel gating kinetics were analyzed using Clampfit (Axon Instruments, Sunnyvale, CA) and Igor software (Wavemetrics, Lake Oswego, OR). Data were presented as mean ± SE (median), and comparisons were made using nonparametric test (Mann-Whitney test) with $P<0.05$ considered significant. The authors had full access to and take full responsibility for the integrity of the data. All authors have read and agree to the manuscript as written.

Results

Clinical Evaluation and Mutation Analysis

Mutational analysis of *SNTA1* in 39 unrelated patients with genotype negative for the previously known LQTS subtypes

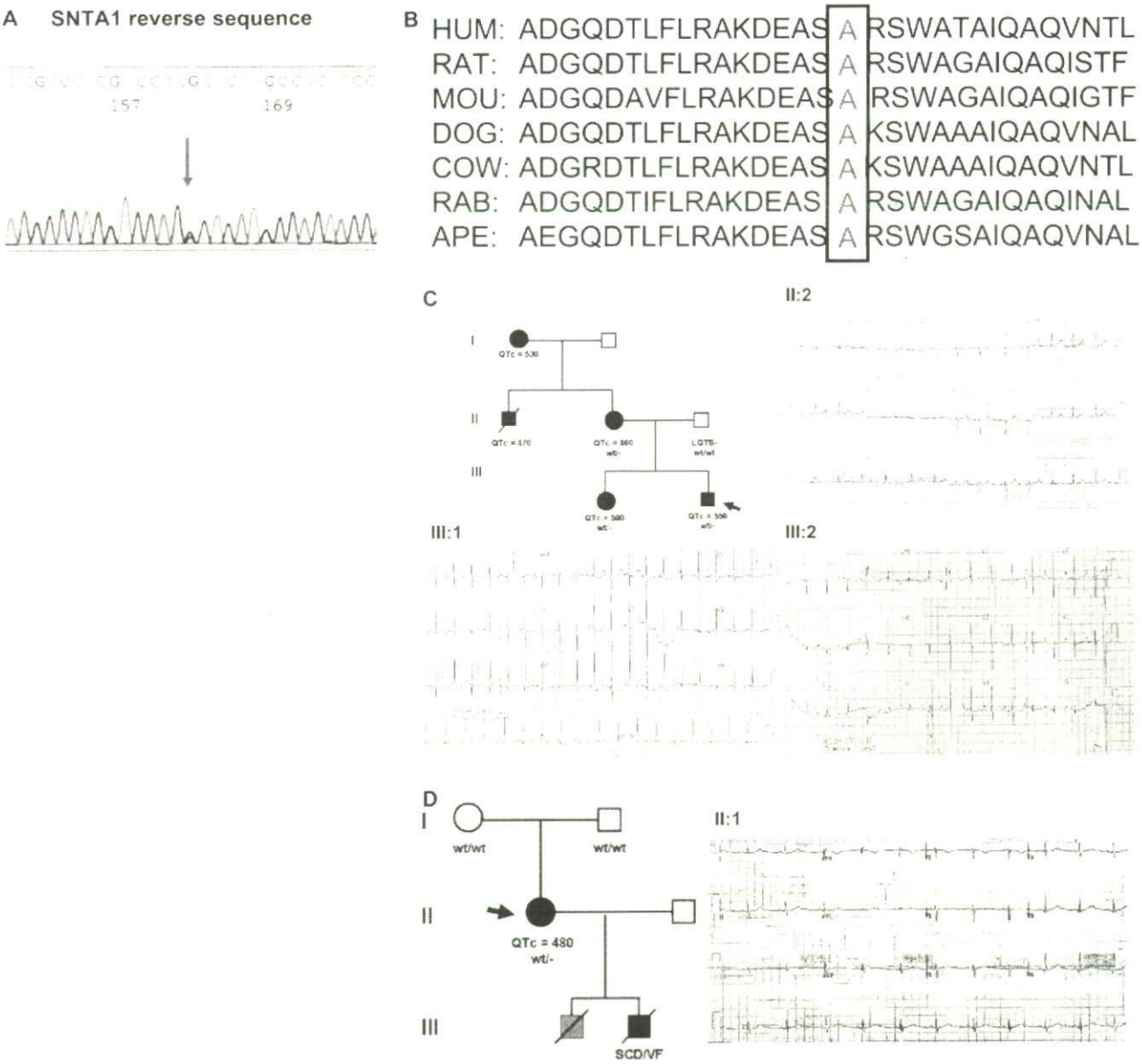

Figure 1. The cytoskeletal protein syntrophin α_1 (SNTA1) mutational analysis in long-QT syndrome (LQTS). Sequencing analysis demonstrates a novel nucleotide variant in *SNTA1* leading to a nonsynonymous change in 3 patients (A) and amino acid conservation analysis of the A257G-SNTA1 variant (B), which modifies a highly conserved amino acid in SNTA1. C, LQT-249 family pedigree and ECG recording showing a pattern with features similar to LQT3 and a prolonged QT interval in proband III: 2, his sister III:1 and his mother II:2 bearing the A257G-SNTA1 mutation. The ECG of the proband demonstrates a prolonged QT interval and late onset T wave.[19] D, LQT-682 family pedigree and ECG recording showing a pattern with features similar to LQT3 and a prolonged QT interval in proband II: 1 bearing the A257G-SNTA1 mutation.

was performed and one novel missense mutation (A257G) was identified in 3 unrelated patients (2 females). This mutation involves a highly conserved residue across several species (Figure 1A and 1B).

The proband is a 17-year-old white male presenting with congenital LQTS. His ECG obtained at 6 hours after birth demonstrated marked QT-prolongation with late onset T-wave pattern (QTc=550 ms, Figure 1C, Table 1, case LQT-249 III: 2). The proband had a syncopal attack at 3 years of age without previous symptoms of prodromal illness, vomiting, diarrhea, fever, or upper respiratory infection. He collapsed while playing in a baby pool after excessive running in a very hot day and remained unconscious for few minutes. The patient underwent Holter monitoring, which showed the average heart rate of 128 bpm (99 to 167) and prolonged QT-intervals (260 to 280 ms). No arrhythmias were documented during the recording. The patient was treated with propranolol. In addition to the SNTA1 mutation, a second variant was identified in KCNQ1 (IVS7+5G>A), which is present in all affected members along with the SNTA1 mutation. Although this variant is of unknown significance, computer predictions analyzed in our labora-

Table 1. Demographics of the Long-QT (LQT) Syndrome Patients

Case No.	Gene Analysis	Age/Sex	Race	Symptom	Onset Age	ECG	
						QTc, ms	T-Wave Morphology
LQT-249-II:1	NA	25†/M	W	Syncope/SCD	UK	470	NA
LQT-249-II:2	A257G	45/F	W	None		460	Asymmetric peaked
LQT-249-III:1	A257G	13/F	W	None		500	Inverted
LQT-249-III:2*	A257G	17/F	W	Syncope with pulmonary arrest	3	550	Late onset
LQT-682*	A257G	37/F	W	Recurrent seizures		480	NA
LQT-755*	A257G	27/F	W	None		480	NA

*Proband; †age at SCD.
W indicates white; SCD, sudden cardiac death; UK, unknown.

tory, using the http://www.fruitfly.org/seq_tools/splice.html software,[20] suggests the possible creation of a cryptic splicing site leading to an in-frame insertion of 25 amino acids in one of the KCNQ1 alleles. This suggests that the KCNQ1 variant may add to the clinical phenotype caused by SNTA1.

A257G mutation was also identified in the proband's sister (subject III:1) and mother (subject II:2). Both of them have been apparently healthy. The sister's ECG obtained at birth showed QT-prolongation (QTc: 500 ms) with normal T-wave pattern in $V_{1\ to\ 3}$ and inverted T-waves in $V_{1\ to\ 6}$. Her Holter ECG demonstrated normal sinus rhythm, no arrhythmias, and prolonged QT intervals. The mother's ECG obtained at 27 years of age showed mild QT prolongation with asymmetrical peaked T-wave pattern (QTc=460 ms; Figure 1C). The proband's maternal uncle died suddenly at age 25 during physical exertion. He had prior history of syncope and prolonged QT interval (QTc=470 ms). No autopsy sample was available to us. The ECG and genetic screening of the proband's father (Figure 1C; Table 1) did not show any abnormalities.

The A257G was also identified in a 37-year-old and a 27-year-old unrelated female with unremarkable family history of either LQTS or sudden cardiac death. Both probands showed QT-prolongation at baseline ECG (QTc=480 ms). Their parents' ECG and genetic screening analysis did not show any abnormalities, consistent with de novo genetic change.

Subject LQT-682 was identified subsequently to screening after her 11-year-old son died suddenly because of ventricular fibrillation registered at the time of the code at the hospital where he was visiting the brother admitted for a car accident. The autopsy findings were negative for structural heart diseases and led to the diagnosis of suspected LQTS, but no sample was available to us. LQT-682 proband had a long-standing history of seizure disorder with normal seizure workup and positive EEG. The proband was treated with phenytoin for her seizure since she was 12-years-old.

The ECG (Figure 1D) and Holter ECG were obtained in the absence of β-blockers but in the presence of phenytoin, and they demonstrated intermittent QT prolongation. Echocardiography assessment was normal. Analysis of 400 ethnic-matched control alleles did not identify the A257G mutation.

Immunostaining

HEK-293 cells stably expressing Flag-tagged $hNa_v1.5$ and GFP-tagged WT-SNTA1 were fixed and stained with anti-Flag antibody. Figure 2A demonstrates that the green fluorescence (SNTA1, middle panel) and red fluorescence (hNav1.5, right panel) when merged give the orange-yellow areas, suggesting colocalization of hNav1.5 and SNTA1, consistent with possible association in a protein complex.

Coimmunoprecipitation Assay of $hNa_v1.5$ and SNTA1

Previous studies showed that the PDZ domain of SNTG2, highly homologous to SNTA1, binds the C-terminal domain of $Na_v1.5$ and affect its gating kinetics.[16] Therefore, we performed coimmunoprecipitation assay using HEK-293 cells stably expressing Flag-tagged $hNa_v1.5$ and transiently transfected with either GFP-tagged WT- or A257G-*SNTA*.

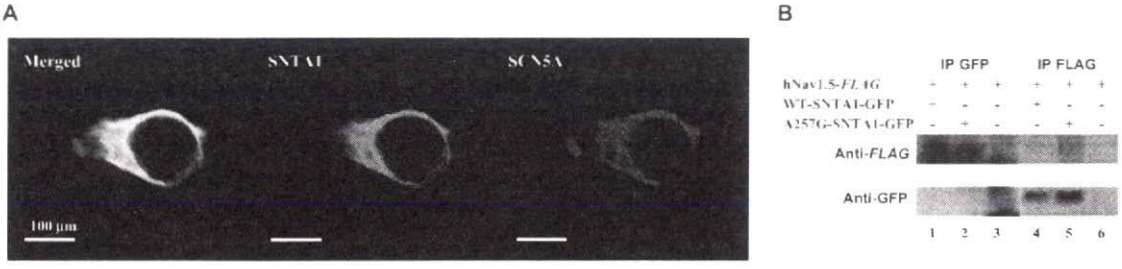

Figure 2. $hNa_v1.5$ and cytoskeletal protein syntrophin-α_1 (SNTA1) may form a protein complex in HEK-293 cells. A, Immunohistochemical staining: The left panel shows the merged images of green fluorescence (mid) and red fluorescence (right) images. The green fluorescence depicts the GFP-tagged SNTA1 and the red fluorescence depicts the Flag-tagged $hNa_v1.5$. B, Coimmunoprecipitation assays. IP indicates immunoprecipitants; (+), transfected with the genes indicated in the left column; (−) nontransfected with the genes.

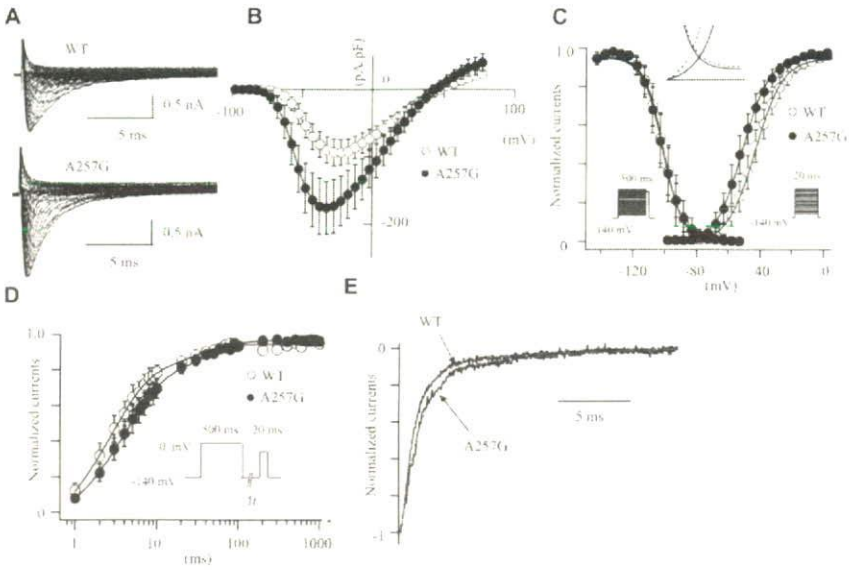

Figure 3. The effects of wild-type cytoskeletal protein syntrophin-α_1 (WT-SNTA1) and A257G-SNTA1 on hNa$_v$1.5 in HEK-293 cells. A, Superimposed whole-cell current traces induced by a step-pulse protocol from a holding potential of −140 mV. B, I-V relationships. C, Voltage-dependence of peak conductance and steady-state fast inactivation. Conductance $G(V)$ was calculated by the equation: $G(V) = I/(V_m - E_{rev})$, where I is the peak currents, E_{rev} is the measured reversal potential, V_m is the membrane potential. The normalized peak conductance was plotted as a function of membrane potentials. Steady-state inactivation was estimated by prepulse protocols (500 ms) from a holding potential of −140 mV. The normalized peak currents were plotted as a function of membrane potentials. Steady-state activation and inactivation were fitted with the Boltzmann equation: $y = [1 + \exp((V_h - V_m)/k)]^{-1}$, where y represents variables; V_h, midpoint; k, slope factor; V_m, membrane potential. The inset indicates the magnified illustration of the window currents. The solid lines represent WT-SNTA1, and the dotted lines represent A257G-SNTA1. D, Recovery from the fast-inactivation estimated by a double pulse protocol. Cells were depolarized at 0 mV for 500 ms from a holding potential of −140 mV, then stepped to −140 mV for various durations before the second pulse (20 ms at −20 mV). The fractional recovery was calculated as the ratio of peak currents at the second pulse. The recovery time course was fitted with a double exponential function: $I(t)/I_{max} = C - A_f \times \exp(-t/\tau_f) - A_s \times \exp(-t/\tau_s)$, where t is the recovery time, A_f and A_s are the fractions of fast and slow components, τ_f and τ_s are the time constants of fast and slow components of recovery. E, Macroscopic current decay was fit with a double exponential function: $I(t)/I_{max} = C - A_f \exp(-t/\tau_f) - A_s \exp(-t/\tau_s)$, where I_{max} is the peak current, t is the time, A_f and A_s are the fractions of fast and slow components, τ_f and τ_s are the time constants of fast and slow components, respectively. The data were represented as mean ± SE.

The anti-GFP antibody detected SNTA1 (87 kDa) in the coimmunoprecipitants with the anti-Flag antibody (Figure 2B, lanes 4 and 5), whereas the anti-Flag antibody detected hNa$_v$1.5 (260 kDa in the coimmunoprecipitants with the anti-GFP (Figure 2B, lanes 1 and 2) for both WT-SNTA1 and A257G-SNTA1, suggesting that human SNTA1 can physically interact with hNa$_v$1.5 and that perturbations in SNTA1 might alter hNa$_v$1.5 function.

Electrophysiological Experiments

Figure 3A shows the superimposed whole-cell current traces obtained from HEK-293 cells stably expressing consistent hNa$_v$1.5 currents and transiently transfected with WT- or A257G-*SNTA1*. Figure 3B shows the current–voltage (I-V) relationships and demonstrates peak current densities nearly twice as large in the cells expressing A257G-SNAT1 compared with WT. In addition, A257G-SNAT1 shifted the onset and peak of the currents toward more negative potentials by 10 mV compared with the WT. Figure 3C shows the effects of A257G-SNAT1 on the voltage-dependent kinetics of steady-state activation and inactivation. The half maximal voltage of the steady-state activation (V_h) was shifted leftward by 8.3 mV in the cells expressing A257G-SNAT1. The slope factor (k) was not affected by A257G-SNAT1. Steady-state inactivation was examined by a prepulse protocol. The normalized currents were plotted as a function of the membrane potentials and fitted by the Boltzman equation. Voltage-dependent inactivation kinetics were not significantly affected by A257G-SNAT1. The leftward shift of steady-state activation without shift of the inactivation kinetics increased the window currents (Figure 3C, inset). These biophysical parameters were also studied in the presence of β_1-subunit of the human cardiac sodium channel (hβ_1): hβ_1 did not significantly modulate the effects of A257G-SNTA1 on the hNa$_v$1.5 gating kinetics (Table 2).

The recovery time from fast inactivation was studied using a 2-pulse protocol. Figure 3D shows the fraction of channels that recovered from the fast inactivation. The data were fitted by a double-exponential equation: the fast components of the time constant (τ_f) were significantly slower in the cells expressing A257G-SNTA1 than WT. The slow components of the time constant (τ_s) and the fraction of fast and slow components were comparable between the WT-SNTA1 and the A257G-SNTA1.

Delay of sodium current decay and generation of sustained sodium currents have been proposed as the pathophysiological mechanisms responsible for the LQT3 phenotype. We estimated the time course of whole-cell current decay and the late sodium currents. Because the I-V curve was shifted, the comparison of the current decay at a same membrane potential might not simply express the time-dependent kinetics. The decay of the peak sodium currents was analyzed with a double exponential fit. Figure 3E shows that A257G-SNTA1 slightly delayed the macroscopic current decay compared with the WT-SNTA1. Although the slow component of time constant was comparable between WT-SNTA1 and A257G-SNTA1, A257G-SNTA1 significantly slowed the fast component of time constant (Table 2). The late sodium currents were evaluated by a long depolarization pulse (2000 ms at −20 mV from a holding potential of −140 mV) using 30 μmol/L tetrodotoxin (TTX). No TTX-sensitive sustained currents were detected in the cells expressing WT-SNTA1

Table 2. Effects of Wild Type (WT) and A257G-SNTA1 on the $Na_v1.5$ Gating Kinetics

	HEK Without β1 Subunit			HEK With β1 Subunit			Neonatal Cardiomyocyte		
	WT	A257G	*P*	WT	A257G	*P*	WT	A257G	*P*
Current density (pA/pF)	−97.8±9.1 (−95.4)	−179.6±18.4 (−182.0)**	0.000	−151.0±25.4 (−140.7)	−336.9±70.0 (−356.7)*	0.018	−316.3±51.1 (−305.7)	−517.5±70.7 (−567.5)*	0.041
n	15	13		12	9		6	6	
Activation									
V_h, mV	−43.5±1.5 (−44.0)	−51.7±1.6 (−51.5)**	0.002	−43.1±1.3 (−42.7)	−50.8±1.5 (−48.9)**	0.001	−47.9±1.7 (−48.4)	−57.3±3.1 (−55.0)*	0.015
k	7.87±0.31 (7.47)	7.91±0.62 (7.49)	0.892	8.80±0.47 (8.98)	8.22±0.24 (8.10)	0.464	7.56±0.37 (7.54)	7.06±0.14 (7.09)	0.24
n	15	13		12	9		6	6	
Fast-inactivation									
V_h, mV	−97.4±1.8 (−96.7)	−101.3±2.0 (−102.1)	0.190	−104.6±7.7 (−102.8)	−105.9±5.8 (−106.0)	0.430	−91.9±2.3 (−91.2)	−91.4±3.1 (−92.1)	0.943
k	5.18±0.19 (5.39)	5.44±0.19 (5.49)	0.740	5.47±0.17 (5.59)	5.59±0.23 (5.76)	0.650	6.43±0.26 (6.71)	7.10±0.13 (6.92)	0.065
n	12	11		13	14		8	5	
Recovery from fast-inactivation									
τ_f, ms	2.92±0.30 (2.59)	4.33±0.56 (3.63)*	0.033						
τ_s, ms	33.43±4.57 (29.86)	41.34±2.14 (40.93)	0.094						
A_f, %	93.4±3.6 (91.6)	87.2±2.8 (87.46)	0.169						
A_s, %	20.4±2.7 (19.8)	23.4±1.8 (22.09)	0.169						
n	13	14							
Current decay									
τ_f, ms	0.92±0.04 (0.94)	1.06±0.04 (1.01)*	0.033				0.80±0.07 (0.74)	1.12±0.08 (1.12)*	0.026
τ_s, ms	8.57±0.99 (7.76)	8.97±1.00 (9.99)	0.586				5.90±1.78 (3.53)	4.23±0.43 (3.96)	0.589
n	15	13					6	6	

V_h indicates midpoint voltage of maximal activation/inactivation; *k*, slope factor; τ_f and τ_s, time constants of fast and slow components of recovery; A_f and A_s, fractions of fast and slow components; n, No. of patches. Numbers in parentheses represent the median of data.

*$P<0.05$; **$P<0.01$ versus WT.

and A257G-SNTA1 (data not shown). Table 2 summarizes the effects of WT-SNTA1 and A257G-SNTA1 on the $Na_v1.5$ gating kinetics.

Because the cellular environment of HEK-293 cells might be far different from myocardial cells, we studied the effects of WT-SNTA1 and A257G-SNTA1 on $Na_v1.5$ in neonatal rat cardiomyocytes. The cardiomyocytes were isolated from neonatal rats (3 to 5 days old) and transfected with GFP-tagged WT-*SNTA1* and the A257G-*SNTA1* by using the Nucleofector. The cardiomyocytes showing green fluorescence were used for the patch-clamp experiments. In native cardiomyocytes, A257G-SNTA1 increased the peak sodium currents and altered the kinetics consistently with that observed in HEK-293 cells. Figure 4A shows the representative whole-cell current traces obtained from the cardiomyocytes transiently transfected with either WT-SNTA1 or A257G-SNTA1. Figure 4B shows the I-V relationships. The peak current densities were significantly larger (1.6 fold) in cells expressing A257G-SNTA1 compared with the WT. The onset and peak of the currents of the I-V relationships were shifted toward negative by approximately 10 mV in cells expressing the A257G-SNTA1 compared with WT. Figure 4C shows the effects of A257G-SNTA1 on the voltage-dependency of the steady-state activation and the inactivation. The V_h of activation curve was shifted leftward by 9.4 mV in the cells transfected with A257G-SNTA1; on the contrary, voltage-dependent inactivation kinetics were not significantly affected by A257G-SNTA1. The persistent sodium currents were examined using a long depolarization pulse protocol (Figure 4D). The 30 μmol/L TTX-sensitive persistent sodium currents were comparable between the WT and the A257G mutant (percentage over the peak currents: WT, 0.25±0.09%, n=4; A257G, 0.22±0.04%, n=4, NS). Figure 4E demonstrates that A257G-SNTA1 delayed the macroscopic current decay (peak currents) compared to the WT-SNTA1. Although the slow component of time constant was comparable be-

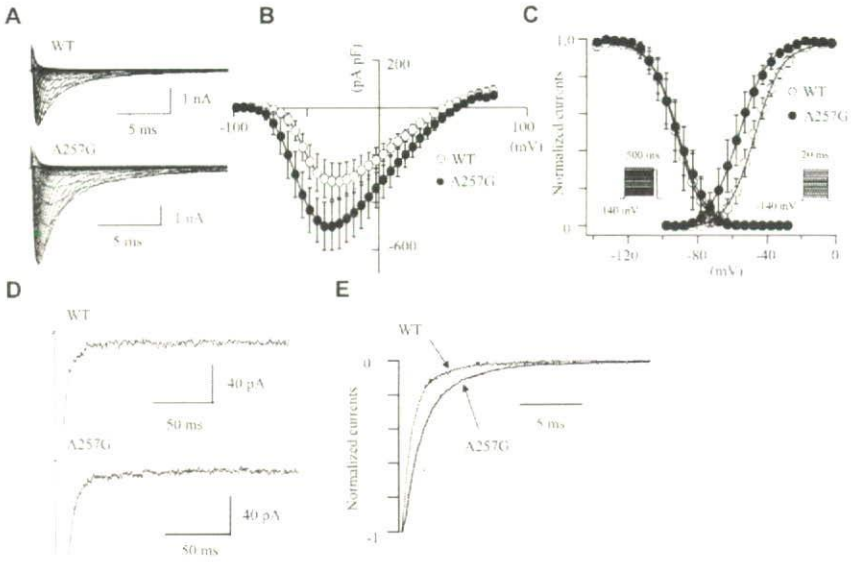

Figure 4. The effects of wild-type cytoskeletal protein syntrophin-α_1 (WT-SNTA1) and A257G-SNTA1 on Na$_v$1.5 in neonatal rat cardiomyocytes. A, Superimposed whole-cell current traces induced by a step-pulse protocol from a holding potential of −140 mV. B, I-V relationships. C, Voltage-dependence of peak conductance and steady-state fast inactivation. D, Magnified current traces of the tetrodotoxin-sensitive late sodium currents induced by a long depolarization-pulse protocol (2000 ms at −20 mV from a holding potential of −140 mV). The dotted lines indicate zero current levels. E, Macroscopic current decay was fit with a double exponential function. The data were represented as mean±SE.

tween WT and mutant SNTA1, A257G-SNTA1 significantly increased the fast component of the time constant (Table 2).

Discussion

Until recently, the pathophysiological mechanisms of inherited arrhythmias were thought to stem merely from primary alterations in ion channels leading to the term "ion channelopathies." However, this paradigm has been challenged by the identification of altered channel-interacting proteins, which can directly modify ion channel functions. In particular, our recent finding demonstrating that caveolin-3 (which cofractionates with dystrophin and the dystrophin glycoprotein complex: DGC) binds Na$_v$1.5 in human heart and if mutated leads to LQTS[5] has focused our attention on the other DGC proteins such as SNTA. SNTA1 is an integral part of the DGC, and regulates the Na$_v$1.5 by forming a multiprotein complex through its direct binding to dystrophin.[21] Our study, for the first time, demonstrates that alteration of SNTA1 can affect the Na$_v$1.5 gating kinetics, leading to the LQTS phenotype.

How Does A257G-SNTA1 Affect the Gating Kinetics of Na$_v$1.5?

A257G-SNTA1 caused gain-of-function of the Na$_v$1.5 through the leftward shift of the activation curve by 8 to 9 mV without shift of the inactivation curve, which might increase the channel availability. The extent of this shift is equal to or larger than previously reported values for *SCN5A* mutations (N1325S, L619F; Figures 3C and 4C).[22,23] In addition, the subtle but significant delay of the fast component of whole-cell current decay (Figures 3E and 4E) and the significantly larger peak current density for A257G-SNTA1 might contribute to an increase of total inward currents.

Ou et al reported that SNTG2, which is highly homologous to SNTA1, can attenuate sodium current densities and shift the voltage-dependent activation kinetics compared with the control.[16] Therefore, it is possible that WT-SNTA1 also attenuates sodium currents, whereas A257G-SNTA1 abolished the ability of WT-SNTA1 to decrease the currents. To prevent the endogenous gene expression level affecting the comparison of the current densities in a transiently transfection system, we established stable HEK-293 cell lines that generate consistent sodium current densities from one single clone, and we transfected them with WT-SNTA1 and A257G-SNTA1 by consistent protocols. Therefore, it is reasonable to speculate that A257G-SNTA1 might increase the open-probability of the channel compared with the WT. Although single-channel recordings need to be studied to elucidate the detail underlying mechanisms, our data indicate that these biophysical modifications by the A257G-SNTA1 can cause gain of function of the cardiac sodium channels in comparison with the WT-SNTA1.

How Does SNTA1 Interact With Na$_v$1.5?

Previous studies demonstrated that the PDZ domain of syntrophins (human SNTG2 and rodent SNTA1) can bind to the C-terminal domain of cardiac sodium channels (hNa$_v$1.5 and rodent Skm2).[15,16] Our study demonstrated that human SNTA1 can directly interact with hNa$_v$1.5 (Figure 2B), which is consistent with these reports and suggests direct protein-protein interaction as the mechanism by which A257G-SNTA1 modifies the hNa$_v$1.5 function.

The previous study using the dystrophin-deficient *mdx* mice suggested that the syntrophin-dystrophin complex plays critical roles in the regulation of the sodium channel gating kinetics, as well as the ECG phenotype (conduction disturbances and QT-prolongation).[24] Therefore, even secondary alterations of the DGC may result in primary hNa$_v$1.5 defects via SNTA1 in cardiomyocytes. In addition, the effect of A257G-SNTA1 on hNa$_v$1.5 in HEK-293 cells demonstrates that SNTA1 plays a key role in hNa$_v$1.5 regulation. Further studies using genetically engineered animal models and addressing the detailed mechanism of Na$_v$1.5 function regulation by SNTA1 and the involvement of other syntrophin